J Neurophysiol 99: 426–441, 2008.
First published December 19, 2007; doi:10.1152/jn.00940.2007.

Presynaptic Release Probability Is Increased in Hippocampal Neurons From ASIC1 Knockout Mice

Jun-Hyeong Cho and Candice C. Askwith
Department of Neuroscience, The Ohio State University, Columbus, Ohio

Submitted 20 August 2007; accepted in final form 12 December 2007

Cho J-H, Askwith CC. Presynaptic release probability is increased in hippocampal neurons from ASIC1 knockout mice. *J Neurophysiol* 99: 426–441, 2008. First published December 19, 2007; doi:10.1152/jn.00940.2007. Acid-sensing ion channels (ASICs) are H^+-gated channels that produce transient cation currents in response to extracellular acid. ASICs are expressed in neurons throughout the brain, and ASIC1 knockout mice show behavioral impairments in learning and memory. The role of ASICs in synaptic transmission, however, is not thoroughly understood. We analyzed the involvement of ASICs in synaptic transmission using microisland cultures of hippocampal neurons from wild-type and ASIC knockout mice. There was no significant difference in single action potential (AP)–evoked excitatory postsynaptic currents (EPSCs) between wild-type and ASIC knockout neurons. However, paired-pulse ratios (PPRs) were reduced and spontaneous miniature EPSCs (mEPSCs) occurred at a higher frequency in ASIC1 knockout neurons compared with wild-type neurons. The progressive block of NMDA receptors by an open channel blocker, MK-801, was also faster in ASIC1 knockout neurons. The amplitude and decay time constant of mEPSCs, as well as the size and refilling of the readily releasable pool, were similar in ASIC1 knockout and wild-type neurons. Finally, the release probability, which was estimated directly as the ratio of AP-evoked to hypertonic sucrose-induced charge transfer, was increased in ASIC1 knockout neurons. Transfection of ASIC1a into ASIC1 knockout neurons increased the PPRs, suggesting that alterations in release probability were not the result of developmental compensation within the ASIC1 knockout mice. Together, these findings demonstrate that neurons from ASIC1 knockout mice have an increased probability of neurotransmitter release and indicate that ASIC1a can affect presynaptic mechanisms of synaptic transmission.

INTRODUCTION

Acid-sensing ion channels (ASICs) are voltage-independent cation-permeable ion channels activated by extracellular acidosis (Krishtal 2003; Waldmann 2001; Wemmie et al. 2006). These H^+-gated channels are members of the degenerin/epithelial Na^+ channels (DEG/ENaC) family (Kellenberger and Schild 2002). Four ASIC genes encode at least six subunits (ASIC1a, 1b, 2a, 2b, 3, and 4) through alternative splicing. ASIC subunits are expressed in central and peripheral neurons, and the characteristics of H^+-gated currents are determined by the ASIC subunits expressed within the cell. ASIC1a, ASIC2a, and ASIC2b are expressed throughout the brain with particularly high abundance in the cerebral cortex, hippocampus, amygdala, olfactory bulb, and the cerebellum (Garcia-Anoveros et al. 1997; Lingueglia et al. 1997; Price et al. 1996; Waldmann et al. 1996, 1997). ASIC1a forms not only heteromeric channels with ASIC2a, but also Ca^{2+}-permeable homomeric channels (Askwith et al. 2004; Bassilana et al. 1997; Benson et al. 2002; Gao et al. 2007; Hesselager et al. 2004; Yermolaieva et al. 2004). ASIC1a is enriched in synaptosomal fractions and expressed in dendritic spines (Hruska-Hageman et al. 2002; Wemmie et al. 2002). ASIC1 knockout mice display impaired spatial learning, eye-blink conditioning, and fear conditioning (Wemmie et al. 2002, 2003). In turn, transgenic mice overexpressing ASIC1a exhibit enhanced fear conditioning (Wemmie et al. 2004). Together, these observations suggest that ASIC1a plays a role in synaptic transmission.

Wemmie et al. (2002) performed extracellular field potential recordings of hippocampal slices and observed that hippocampal CA1 long-term potentiation (LTP) was impaired in ASIC1 knockout mice. Specifically, *N*-methyl-D-aspartate receptor (NMDAR) activation during high-frequency stimulation was reduced in hippocampal CA3–CA1 synapses of ASIC1 knockout mice. The authors hypothesized that protons released from synaptic vesicles activate postsynaptic ASICs, which depolarize the postsynaptic membrane and facilitate activation of NMDARs by relieving Mg^{2+} block (Wemmie et al. 2002). Depolarization-induced removal of Mg^{2+} block from the NMDAR is usually mediated by the activation of α-amino-3-hydroxy-5-methyl-4-isoxazolepropionic acid receptors (AMPARs). In specific situations, such as silent synapses that express few functional AMPARs in the postsynaptic membrane, ASICs might induce NMDAR activation and thereby facilitate LTP. ASIC-mediated H^+-gated current, however, has not yet been observed during high-frequency stimulation, and inhibition of ASIC channels does not appear to affect postsynaptic currents (Alvarez de la Rosa et al. 2003). These results suggest that ASICs may influence synaptic transmission through an alternate mechanism.

In this study, we examined the role of ASICs in synaptic transmission using microisland cultures of hippocampal neurons from wild-type and ASIC knockout mice. Solitary neurons in microisland culture are synaptically isolated from other neurons; monosynaptic connections (autapses) form between the axon and dendrites of the same neuron (Bekkers and Stevens 1991). This preparation allows a detailed analysis of presynaptic and postsynaptic parameters of synaptic transmission in the absence of complex polysynaptic circuitry (Bekkers and Stevens 1991). Microisland cultures have been widely used for electrophysiologic studies of synaptic transmission on both cellular and molecular levels (Chavis and Westbrook 2001; Rhee et al. 2002; Rosenmund and Stevens 1996; Wierda et al. 2007). Using this method, we determined that the prob-

Address for reprint requests and other correspondence: C. C. Askwith, Department of Neuroscience, The Ohio State University, 333 West 10th Avenue, Columbus, OH 43210 (E-mail: askwith.1@osu.edu).

The costs of publication of this article were defrayed in part by the payment of page charges. The article must therefore be hereby marked "*advertisement*" in accordance with 18 U.S.C. Section 1734 solely to indicate this fact.

ability of neurotransmitter release is increased in neurons from ASIC1 knockout mice, suggesting that ASIC1a can influence glutamatergic synaptic transmission through presynaptic mechanisms.

METHODS

Microisland culture of hippocampal neurons

Primary hippocampal neuron cultures were prepared using previously published methods (Askwith et al. 2004; Cho and Askwith 2007). Briefly, hippocampi were dissected from postnatal day (P) 0–P1 pups, freed from extraneous tissue, and cut into pieces. ASIC1 and ASIC2 knockout mice develop and breed normally, and there are no overt abnormalities in brain morphology (Price et al. 2000; Wemmie et al. 2002). Hippocampal tissue was transferred into Leibovitz's L-15 medium containing 0.25 mg/ml bovine serum albumin and 0.38 mg/ml papain, and incubated for 15 min at 37°C with 95% O_2-5% CO_2 gently blown over the surface of the medium. After incubation, the hippocampal tissue was washed three times with mouse M5-5 medium (Earle's minimal essential medium with 5% fetal bovine serum, 5% horse serum, 0.4 mM L-glutamine, 16.7 mM glucose, 5,000 U/l penicillin, 50 mg/l streptomycin, 2.5 mg/l insulin, 16 nM selenite, and 1.4 mg/l transferrin) and triturated. For conventional mass cultures, a collagen solution containing 0.5 mg/ml rat tail collagen in 1:1,000 acetic acid was spread onto 10-mm glass coverslips. For microisland cultures, a microatomizer was used to spray a fine mist of collagen solution onto the coverslips (Bekkers and Stevens 1991). The collagen was allowed to dry completely and then the coverslips were exposed to UV light for 1 h. Hippocampal cells were plated on coverslips in 24-well dishes in M5-5 media at a density of 500,000 cells per well for mass culture and 250,000 cells per well for microisland culture. After 48–72 h, 10 μM cytosine β-D-arabinofuranoside was added to inhibit glial proliferation. Neurons in conventional mass culture were used from 9 to 13 days in culture and neurons in microisland culture were used from 12 to 19 days in culture. Multiple breeding pairs of ASIC1 knockout (three pairs), ASIC2 knockout (three pairs), and wild-type (composed of three pairs of wild-type siblings of ASIC1 and three pairs of wild-type siblings of ASIC2 knockout) mice were used to produce neonatal pups. No difference was observed in H^+-gated currents or postsynaptic responses between wild-type neurons from the ASIC1 or ASIC2 knockout mouse lines.

Transfection of primary hippocampal neurons

Human ASIC1a cDNA (GenBank Accession Number NM_001095) was cloned into the pcDNA3.1 expression vector (Invitrogen, Carlsbad, CA). Hippocampi were dissected from ASIC1 knockout pups of P0–P1 as before except that hippocampal cells were transfected with the ASIC1a or vector just prior to plating. Briefly, dissociated hippocampal cells were split into two groups from the same preparation (3–4 million cells each group), suspended in 100 μl of Nucleofector Solution from the Basic Nucleofector Kit (Amaxa, Gaithersburg, MD), and mixed with 1 μg of pEGFP-C1 (Clontech, Mountain View, CA) as well as 2 μg of either the ASIC1a construct or vector alone (pcDNA3.1). Hippocampal cells were electroporated with the Nucleofector II (program O-05, Amaxa) and plated on collagen-spritzed coverslips in 24-well dishes at a density of 500,000–1,000,000 cells per well in M5-5 media. Culture medium was replaced with fresh M5-5 medium 24 h after plating. Cytosine β-D-arabinofuranoside (10 μM) was added 48–72 h after plating. Single neurons on microislands were used for patch-clamping from 14 to 20 days in culture. Transfected cells were identified by green fluorescent protein (GFP) fluorescence and selected for recording using a Nikon TE2000-S epifluorescent microscope. The whole cell configuration was established on isolated neurons with green fluorescence, and acidic solution (pH 6.0) was applied to examine the functional expression of ASIC1a. Because the vast majority of wild-type neurons (51 of 53 neurons) displayed H^+-gated currents in excess of 0.25 nA, we excluded ASIC1a-transfected neurons with green fluorescence and pH 6.0–evoked response $<$0.25 nA. This method ensured that each ASIC1a-transfected neuron included in the study expressed ASIC1a. In the ASIC1a-transfection group, 36% of the neurons with green fluorescence (12 of 33 neurons) displayed typical H^+-gated currents with a peak amplitude $>$0.25 nA. In the vector-transfection group, none of the neurons with green fluorescence displayed transient H^+-gated currents.

Electrophysiology

To record H^+-gated and postsynaptic currents, we used the whole cell voltage-clamp technique. The extracellular solution contained 128 mM NaCl, 5.4 mM KCl, 2 mM $CaCl_2$, 1 mM $MgCl_2$, 5.55 mM glucose, 1 μM glycine, and 0.8 mM HEPES. Unless otherwise indicated, this low concentration of pH buffer (HEPES) was used to facilitate ASIC activation by endogenous acidic fluctuations in pH. Tetramethylammonium hydroxide was used to adjust the pH of the extracellular solution to either pH 7.4 or pH 6.0. An extracellular pH 6.0 solution containing 10 mM HEPES and 10 mM MES as pH buffers was used to evoke H^+-gated currents. The intracellular pipette solution contained 121 mM KCl, 10 mM NaCl, 2 mM $MgCl_2$, 5 mM EGTA, 10 mM HEPES, 2 mM Mg-ATP, and 300 μM Na_3GTP (pH 7.25). For perforated-patch recording, we used the intracellular pipette solution containing 130 mM K-gluconate, 20 mM KCl, 10 mM HEPES, and 0.1 mM EGTA (pH 7.3). The pipette tip was filled with the intracellular solution and back-filled with the solution containing 150 μg/ml of nystatin. Patch electrodes were pulled with a P-97 micopipette puller (Sutter Instrument, Novato, CA) and fire-polished with a microforge (Narishige, East Meadow, NY). Micropipettes with 2–4 MΩ were used for experiments. The membrane potential was held constant at -70 mV. Data were collected at 5 kHz using an Axopatch 200B amplifier, Digidata 1322A, and Clampex 9 (Molecular Devices, Sunnyvale, CA). Neurons were continuously superfused with the extracellular solution from gravity-fed perfusion pipes at a flow rate of about 1 ml/min. Perfusion pipes were placed 250 to 300 μm away from cells, and flow was directed toward the recorded cells to ensure fast solution exchange. There was no significant difference in whole cell membrane capacitance of neurons from the three genotypes (95 $\pm$ 10, 101 $\pm$ 17, 85 $\pm$ 10 pF, n = 24, 10, 22 for wild-type, ASIC1 knockout, and ASIC2 knockout neurons, respectively), suggesting neuron size was not different between genotypes.

H^+-gated currents were evoked by the exogenous application of pH 6.0 extracellular solutions. Desensitization time constant (τ_D) was calculated by fitting the decay phase of H^+-gated currents to the single-exponential equation, $I(t) = I_{max} \exp(-t/\tau_D)$, where I_{max} is the peak amplitude of H^+-gated current at pH 6.0. To record action potential (AP)–evoked whole cell postsynaptic currents, solitary autaptic neurons on microislands were selected and stimulated every 10 s (0.1 Hz) with a transient depolarization of membrane potential from -70 to $+10$ mV for 2 ms. Extracellular solution containing 10 μM 6-cyano-7-nitroquinoxaline-2,3-dione (CNQX) / 50 μM D-2-amino-5-phosphonovaleric acid (AP5) or 30 μM bicuculline was used to determine whether the autaptic neuron was glutamatergic or GABAergic. To isolate AMPAR- or NMDAR-mediated excitatory postsynaptic current (EPSC), we used 1 mM Mg^{2+} or 10 μM CNQX in Mg^{2+}-free solution, respectively. We attained similar results when the AMPAR EPSC was isolated with 50 μM AP5. Decay time constants (τ) of AMPAR EPSC or $GABA_A$ receptor-mediated postsynaptic current ($GABA_AR$ PSC) were calculated by fitting curves of postsynaptic currents to the single-exponential equation, $I(t) = I_{max} \exp(-t/\tau)$, where I_{max} is the peak amplitude of AMPAR EPSC or $GABA_AR$ PSC. To quantify the decay rate of NMDAR

EPSCs, we calculated the weighted mean decay time constant of NMDAR EPSC. NMDAR EPSC curves were fitted to the double-exponential equations, $I(t) = I_f \exp(-t/\tau_f) + I_s \exp(-t/\tau_s)$, where I_f/τ_f and I_s/τ_s are fast and slow components of peak amplitudes and decay time constants of NMDAR EPSC; the weighted mean decay time constants (τ_w) were calculated from the equation, $\tau_w = \tau_f[I_f/(I_f + I_s)] + \tau_s[I_s/(I_f + I_s)]$. Miniature EPSC (mEPSC) and hypertonic (500 mM) sucrose-induced currents were recorded from neurons in conventional mass culture using the extracellular solution containing 1 mM Mg^{2+}, 30 μM bicuculline, and 1 μM tetrodotoxin. Unless otherwise indicated, all reagents were purchased from Invitrogen/Gibco (Carlsbad, CA), Sigma–Aldrich (St. Louis, MO), or Fisher Scientific (Waltham, MA).

Data were analyzed using Clampfit 9 software (Molecular Devices). We analyzed mEPSC using the template search function of Clampfit 9. Data are presented as means ± SE. As appropriate, a two-tailed Student's *t*-test and one-way ANOVA with Bonferroni's simultaneous multiple comparisons were used for statistical analyses and performed with Minitab15 software (Minitab, State College, PA).

RESULTS

H^+-gated currents are altered in ASIC knockout neurons cultured on microislands

In conventional mass-cultured hippocampal neurons, ASIC1a homomultimers and ASIC1a/ASIC2a heteromultimers are responsible for the majority of H^+-gated currents (Askwith et al. 2004). The ASIC1a subunit plays a dominant role, and loss of ASIC1a eliminates H^+-gated currents evoked by pH values >5 (Wemmie et al. 2002; Xiong et al. 2004). The ASIC2a subunit modulates H^+-gated current by forming heteromultimeric channels with ASIC1a that desensitize more rapidly and recover from previous acid applications more quickly compared with homomultimeric ASIC1a channels (Askwith et al. 2004; Benson et al. 2002). To determine whether ASIC1 and ASIC2 have similar roles in microisland culture, we analyzed H^+-gated currents of solitary hippocampal neurons from wild-type, ASIC1 knockout, and ASIC2 knockout mice. Application of acidic extracellular solution (pH 6.0) did not induce a substantial transient current in ASIC1 knockout neurons (Fig. 1, *A* and *B*, peak amplitude = 39 ± 17 pA, $n = 13$, $P < 0.01$, wild-type vs. ASIC1 knockout, one-way ANOVA). By comparison, extracellular application of pH 6.0 solution induced transient inward currents in both wild-type and ASIC2 knockout neurons (Fig. 1, *A* and *B*, peak amplitude = 796 ± 106 pA, $n = 53$ for wild-type, and 1,595 ± 217 pA, $n = 31$ for ASIC2 knockout). The peak amplitude and desensitization time constant (τ_D) of H^+-gated currents were significantly larger in ASIC2 knockout neurons compared with wild-type neurons (Fig. 1, *B* and *C*, $P < 0.01$ for peak amplitude, one-way ANOVA; $P < 0.05$ for desensitization time constants, unpaired *t*-test). Recovery from desensitization was also substantially slower in ASIC2 knockout neurons compared with wild-type neurons (Fig. 1, *A* and *D*, 45 ± 3%, $n = 37$ for wild-type, 17 ± 3%, $n = 31$ for ASIC2 knockout, $P < 0.0001$, unpaired *t*-test). These results are consistent with the loss of ASIC1a/ASIC2a heteromeric channels, which desensitize and recover faster, in the ASIC2 knockout neurons (Askwith et al. 2004; Benson et al. 2002). These results

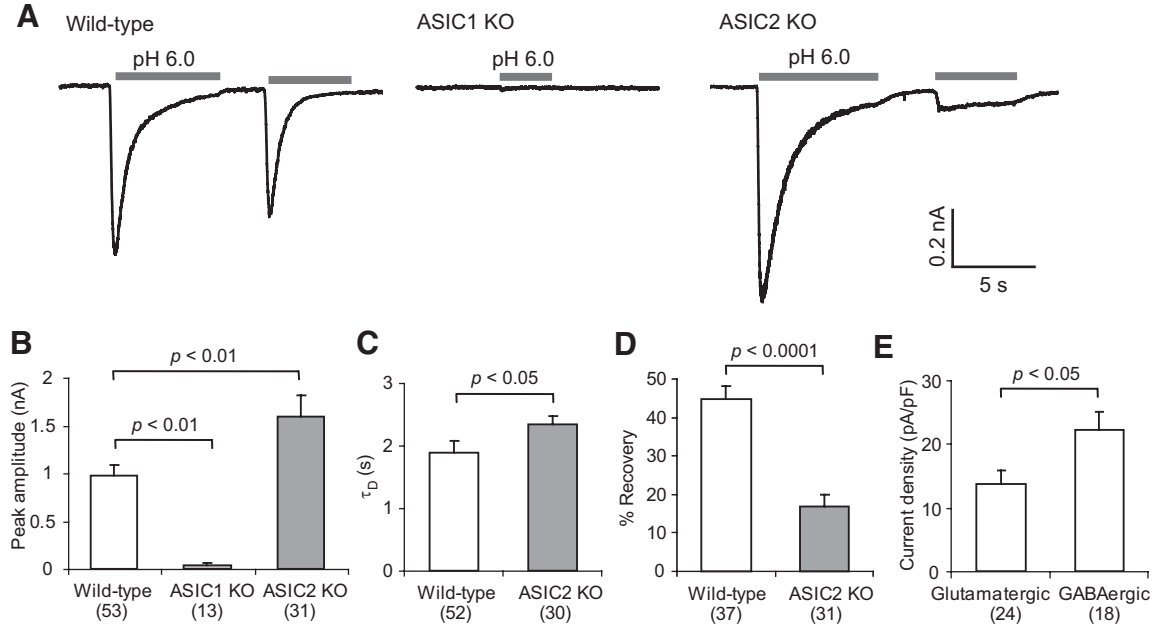

FIG. 1. H^+-gated currents of autaptic neurons in microisland cultures. *A*: representative traces of H^+-gated currents of wild-type, acid-sensing ion channel 1 knockout (ASIC1 KO) and ASIC2 knockout (ASIC2 KO) neurons in microisland culture. To evoke H^+-gated currents, we exchanged the extracellular solution of pH 7.4 to pH 6.0 for 6–7 s (gray bars). To estimate recovery from desensitization, the pH of the extracellular solution was returned to 7.4 for about 2.5 s, and then a second pH 6.0 application was made in wild-type and ASIC2 knockout neurons. *B*: peak amplitude of pH 6.0–induced H^+-gated currents. *C*: the desensitization time constants (τ_D) of H^+-gated current at pH 6.0. *D*: recovery from desensitization was determined by applying 2 pulses of pH 6.0 with an interval of 2.5 s. Recovery was assessed by comparing the peak current amplitude in response to the first pH 6.0 applications to the peak current amplitude of the second pH 6.0 application. *E*: the current density of H^+-gated currents in glutamatergic and GABAergic autaptic neurons from wild-type mice. Current density was calculated by dividing the peak amplitude of pH 6.0–induced current by whole cell membrane capacitance. Numbers in parentheses indicate the numbers of neurons examined. All data in this and subsequent figures are expressed as means ± SE. One-way ANOVA (*B*) and unpaired *t*-test (*C–E*) were used to assess statistical significance.

indicate that ASIC subunits play similar roles in microisland culture and conventional mass culture (Askwith et al. 2004).

Whether a solitary neuron in microisland culture is glutamatergic or GABAergic can be determined by analyzing the AP-evoked postsynaptic current. Extracellular solutions containing CNQX/AP5 or bicuculline were used to identify the autaptic neuron as glutamatergic or GABAergic, respectively. Both glutamatergic and GABAergic autaptic neurons expressed H^+-gated currents in wild-type and ASIC2 knockout neurons. The current density (peak current amplitude divided by whole cell membrane capacitance) of H^+-gated currents was significantly greater in GABAergic neurons than in glutamatergic neurons (Fig. 1*E*, 13.7 ± 2.2 pA/pF, $n = 24$ for glutamatergic neurons, and 22.3 ± 2.7 pA/pF, $n = 18$ for GABAergic neurons, $P < 0.05$, unpaired *t*-test). The desensitization time constant and recovery from desensitization of H^+-gated currents were not different between these two populations of neurons (data not shown). Together, these data indicate that both glutamatergic and GABAergic neurons in microisland culture express H^+-gated channels with biophysical characteristics similar to those of mass-cultured neurons.

Whole cell postsynaptic currents in solitary neurons in microisland culture

To gain insight into the role of ASICs in synaptic transmission, AP-evoked postsynaptic currents of solitary neurons in microisland culture were analyzed using the whole cell voltage-clamp technique. In GABAergic autaptic neurons there was no significant difference in the peak amplitude or decay time constant of $GABA_A$R-mediated postsynaptic current between wild-type and ASIC knockout neurons (Fig. 2, *A* and *B*, peak amplitude = 4.19 ± 0.43, 3.48 ± 0.34, 4.52 ± 0.56 nA, $n = 61$, 48, 32 for wild-type, ASIC1 knockout, and ASIC2 knockout, respectively, $P = 0.27$; decay time constant = 119 ± 24, 132 ± 27, 115 ± 22 ms, $n = 12$, 14, 13 for

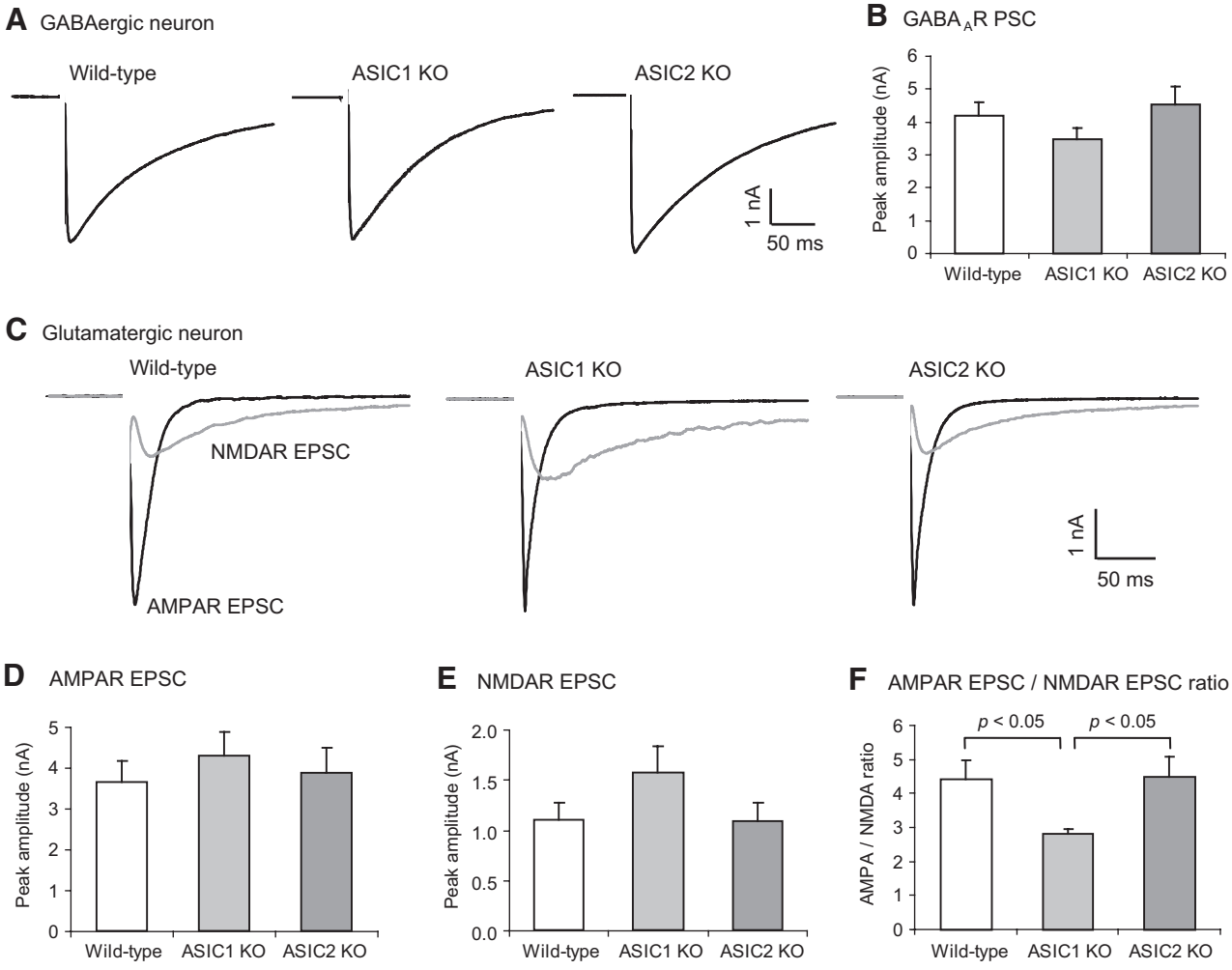

FIG. 2. Whole cell action potential (AP)–evoked postsynaptic currents in GABAergic and glutamatergic autaptic neurons. *A*: representative traces of whole cell $GABA_A$ receptor-mediated postsynaptic current ($GABA_A$R PSC) of wild-type, ASIC1 knockout, and ASIC2 knockout neurons. A 2-ms depolarization to +10 mV from a −70-mV holding potential was used to evoke neurotransmitter release and postsynaptic currents. *B*: quantification of peak amplitude of $GABA_A$R PSC. $n = 62$, 48, and 32 for wild-type, ASIC1 knockout, and ASIC2 knockout. *C*: representative traces of whole cell AMPAR–mediated excitatory postsynaptic current (EPSC, black), and NMDAR–mediated EPSC (gray) of wild-type, ASIC1 knockout, and ASIC2 knockout neurons. AMPAR EPSCs were recorded in the presence of 1 mM Mg^{2+}. NMDAR EPSCs were isolated in Mg^{2+}-free extracellular solution using 10 μM 6-cyano-7-nitroquinoxaline-2,3-dione (CNQX), an AMPAR antagonist. Membrane potential was held at −70 mV. *D–F*: average peak amplitude of the AMPAR EPSCs (*D*), NMDAR EPSCs (*E*), and the average AMPAR EPSC/NMDAR EPSC ratio from individual neurons (*F*). $n = 40$, 42, and 28 for wild-type, ASIC1 knockout, and ASIC2 knockout. One-way ANOVA was used to assess statistical significance.

wild-type, ASIC1 knockout, and ASIC2 knockout, respectively, $P = 0.87$, one-way ANOVA). In glutamatergic autaptic neurons, AMPAR- and NMDAR-mediated EPSCs were individually isolated using either 1 mM Mg^{2+} or 10 μM CNQX, respectively (Fig. 2*C*). Although there was a slight increase in the average peak amplitudes in ASIC1 knockout neurons, there was no significant difference between wild-type and ASIC knockout neurons in the peak amplitudes of either the AMPAR EPSC or NMDAR EPSC (Fig. 2, *D* and *E*, peak amplitude of AMPAR EPSC = 3.65 ± 0.50, 4.29 ± 0.58, 3.87 ± 0.60 nA, $n = 40, 42, 28$ for wild-type, ASIC1 knockout, and ASIC2 knockout, respectively, $P = 0.69$; peak amplitude of NMDAR EPSC = 1.10 ± 0.17, 1.58 ± 0.26, 1.08 ± 0.18 nA for wild-type, ASIC1 knockout, and ASIC2 knockout respectively, $P = 0.17$, one-way ANOVA). There was also no significant difference in the decay time constant of AMPAR or NMDAR EPSC (decay time constant of AMPAR EPSC = 11.4 ± 0.8, 13.3 ± 1.3, 10.6 ± 0.9 ms, $n = 36, 40, 27$ for wild-type, ASIC1 knockout, and ASIC2 knockout respectively, $P = 0.18$; weighted mean decay time constant of NMDAR EPSC = 198 ± 14, 182 ± 9, 155 ± 11 ms, $n = 45, 48, 28$ for wild-type, ASIC1 knockout, and ASIC2 knockout, respectively, $P = 0.07$, one-way ANOVA). To compare the relative contribution of AMPARs and NMDARs to the total EPSC, we recorded both AMPAR and NMDAR EPSCs in the same neurons and calculated the ratio of AMPAR EPSC to NMDAR EPSC. The AMPAR/NMDAR EPSC ratio was significantly smaller in ASIC1 knockout neurons compared with wild-type and ASIC2 knockout neurons (Fig. 2, *C* and *F*, AMPAR EPSC/NMDAR EPSC ratio = 4.41 ± 0.33, 2.82 ± 0.15, 4.52 ± 0.57, $n = 40, 42, 28$ for wild-type, ASIC1 knockout, and ASIC2 knockout, respectively, $P < 0.05$, ASIC1 knockout vs. wild-type or ASIC2 knockout, one-way ANOVA). The fact that ASIC1 knockout neurons displayed a decrease in the AMPAR/NMDAR EPSC ratio could be due to a relative decrease in the peak amplitude of AMPAR EPSC or a relative increase in peak amplitude of the NMDAR EPSC in ASIC1 knockout neurons. Although variability in AMPAR and NMDAR EPSCs between neurons prevented the detection of a statistically significant change in the peak amplitude of AMPAR or NMDAR EPSC, this result suggests that there is a fundamental difference in glutamatergic synaptic transmission in ASIC1 knockout neurons.

ASIC currents are not components of EPSCs

If ASIC currents contribute directly to the postsynaptic current, then loss of H^+-gated currents could explain the altered AMPAR/NMDAR EPSC ratio in the ASIC1 knockout neurons. ASIC1a is enriched in synaptosomal fractions and expressed in dendritic spines, suggesting ASICs play a role at postsynaptic sites (Hruska-Hageman et al. 2002; Wemmie et al. 2002, 2004). The pH inside synaptic vesicles is acidic (pH < 6.0) (Miesenbock et al. 1998) and protons are released from synaptic vesicles during synaptic transmission. Under certain circumstances, such as high-frequency synaptic transmission, these released protons can lower the pH of the synaptic cleft (Krishtal et al. 1987) and affect pH-sensitive ion channel activity. This has been shown for voltage-gated Ca^{2+} channels in retinal cone photoreceptor and bipolar cells (DeVries 2001; Hosoi et al. 2005; Palmer et al. 2003; Vessey et al. 2005). ASIC activation evoked by protons released from synaptic vesicles has not been demonstrated, although spontaneous autocrine release of protons activates endogenous ASIC currents in HEK293 cells (Lalo et al. 2007). Protons released from synaptic vesicles may be rapidly trapped by endogenous pH buffers, and the acute activation of ASICs by protons would likely be for only a short time (Krishtal et al. 1987). Thus protons released during synaptic transmission may activate ASIC1a-containing channels, generating postsynaptic currents in wild-type neurons, which could contribute to the early component of EPSC (AMPAR EPSC). ASIC1 knockout neurons would lack this H^+-dependent current and thus display a smaller AMPAR/NMDAR EPSC ratio. To test this hypothesis, we examined whether ASICs directly contribute to postsynaptic currents.

First, we determined whether ASIC current could be isolated during synaptic transmission. Both AMPAR and NMDAR EPSCs were simultaneously inhibited using 10 μM CNQX and 50 μM AP5 in wild-type glutamatergic neurons on microislands. When both AMPARs and NMDARs were blocked, a small transient residual current was observed in glutamatergic neurons that contributed to the peak AMPAR EPSC (Fig. 3*A*). This current was not significantly different between wild-type and ASIC1 knockout neurons (128 ± 31 pA, $n = 7$ for wild-type neurons; 124 ± 50 pA, $n = 7$ for ASIC1 knockout neurons, $P = 0.96$, unpaired *t*-test). We also recorded both the AMPAR EPSC and the residual current in the same neuron and calculated the ratio of the residual current amplitude to the peak amplitude of the AMPAR EPSC. The ratio was not different between wild-type and ASIC1 knockout neurons (Fig. 3*B*, 4.06 ± 0.77%, $n = 7$ for wild-type neurons; 5.18 ± 0.96%, $n = 7$ for ASIC1 knockout neurons, $P = 0.38$, unpaired *t*-test), suggesting that the contribution of the residual current to peak AMPAR EPSC was not affected by the loss of ASIC1.

We also examined the effect of amiloride (300 μM), a nonspecific ASIC blocker, on residual current and AMPAR EPSCs (Fig. 3, *C* and *E*). H^+-gated currents evoked by exogenous acid application were blocked nearly completely by 300 μM amiloride (Fig. 3*C*). However, the contribution of the residual current to AMPAR EPSCs in wild-type glutamatergic neurons was not affected by amiloride (Fig. 3, *C* and *D*, 3.62 ± 0.80 and 3.30 ± 0.98% before and during amiloride application, respectively, $n = 5$, $P = 0.38$, paired *t*-test). Furthermore, AMPAR EPSCs were not altered by amiloride in either wild-type or ASIC1 knockout neurons (Fig. 3, *E* and *F*, 92.1 ± 4.1% of pretreatment control, $n = 8$, $P = 0.10$, paired *t*-test for wild-type; 99.7 ± 4.6%, $n = 8$, $P = 0.35$, paired *t*-test for ASIC1 knockout; $P = 0.23$, wild-type vs. ASIC1 knockout, unpaired *t*-test). Together, these results indicate that ASIC currents are not components of the EPSC and the altered AMPAR/NMDAR EPSC ratio in ASIC1 knockout neurons cannot be explained by loss of postsynaptic ASIC currents evoked during synaptic transmission. Thus another mechanism is responsible for the decrease in AMPAR/NMDAR EPSC ratio in the ASIC1 knockout neurons.

Exogenous acid application did not alter whole cell postsynaptic currents

Activation of ASIC1a channels could induce changes in AMPAR-, NMDAR-, or $GABA_A$R-mediated postsynaptic cur-

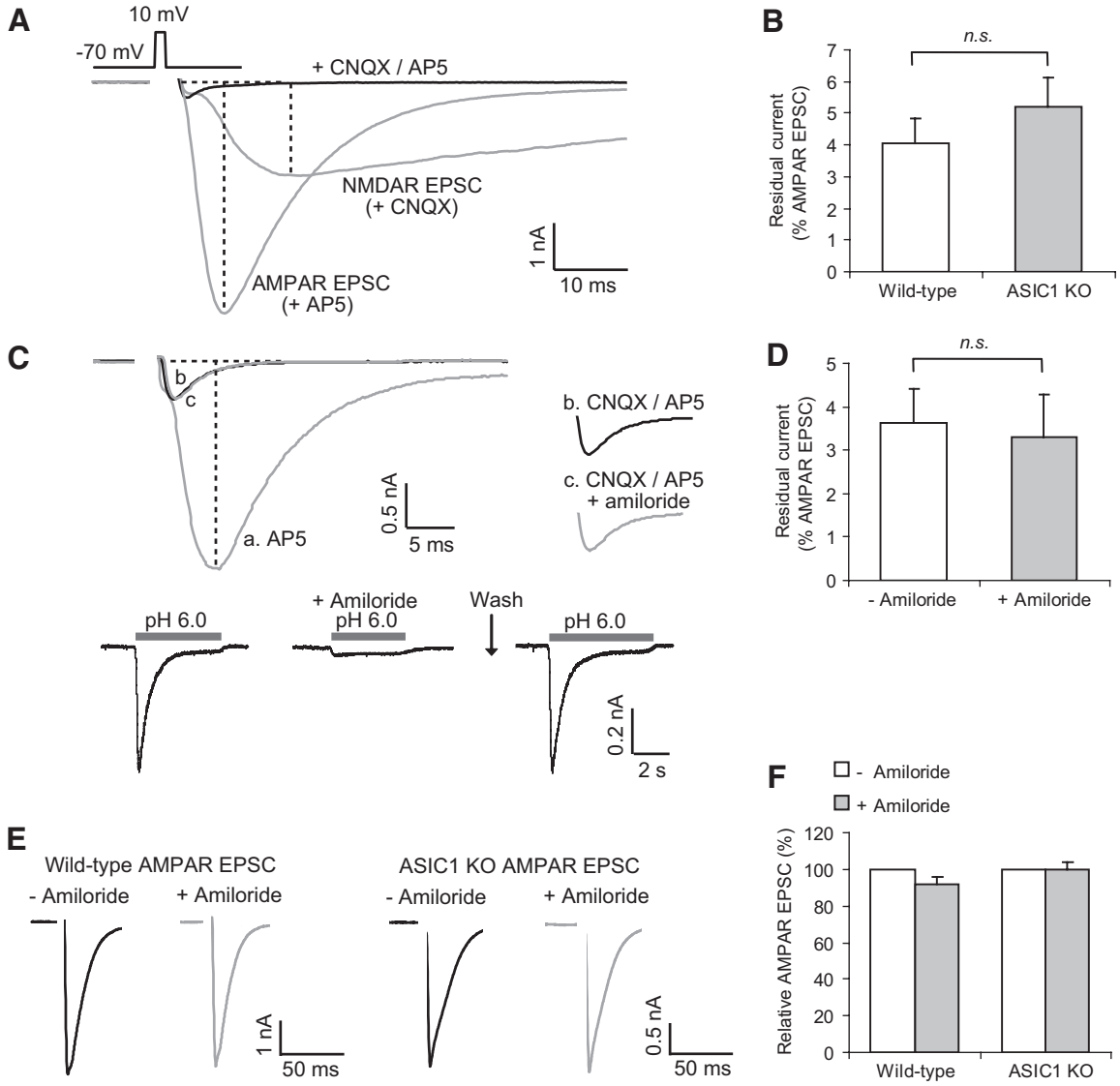

FIG. 3. ASIC currents do not contribute to the peak amplitude of EPSC in glutamatergic autaptic neurons. *A*: representative traces of AMPAR and NMDAR EPSC (*gray traces*) of a wild-type autaptic neuron. In the presence of 10 μM CNQX and 50 μM D-2-amino-5-phosphonovaleric acid (AP5), small residual current was observed (*black trace*). Vertical dotted lines indicate the time of the peak amplitude of AMPAR and NMDAR EPSCs. A voltage step above the traces indicates transient membrane depolarization from −70 to 10 mV for 2 ms used to evoke an AP. *B*: the ratio of the residual current measured in the presence of CNQX and AP5 to the peak AMPAR EPSC in wild-type ($n = 7$) and ASIC1 knockout ($n = 7$) neurons. There is no significant difference in the ratio of residual current to AMPAR EPSC between wild-type and ASIC1 knockout neurons (unpaired *t*-test). *C*: representative traces of AMPAR EPSCs and residual current in the presence of CNQX and AP5 in a wild-type autaptic neuron (*top traces*). AMPAR EPSCs (*a*, *gray trace*) were recorded in the presence of AP5. Residual current (*b*, *black trace*) was isolated using CNQX and AP5 and was not affected by 300 μM amiloride (*c*, *gray trace*). *Bottom traces* show amiloride (300 μM) inhibition of H^+-gated currents evoked by extracellular acid application (pH 6.0, gray bars). *D*: the ratio of the residual current to the AMPAR EPSC before and during amiloride application. Amiloride did not change the ratio significantly ($n = 5$, paired *t*-test). *E*: representative traces of AMPAR EPSCs before (−amiloride, *black traces*) and during 300 μM amiloride application (+amiloride, *gray traces*) in wild-type and ASIC1 knockout neurons. *F*: quantification of the effect of amiloride on AMPAR EPSCs. Current amplitude during amiloride application (+amiloride) was normalized to current amplitude before amiloride treatment (−amiloride). Amiloride did not change the peak amplitude of AMPAR EPSC significantly ($n = 8$, $P = 0.10$ for wild-type, and $n = 8$, $P = 0.65$ for ASIC1 knockout, paired *t*-test).

rents through signal transduction cascades. To test this, we measured whole cell postsynaptic currents before and after activating ASICs with exogenously applied acid. Postsynaptic currents were recorded every 10 s in wild-type autaptic neurons. After the peak amplitude of baseline postsynaptic currents stabilized, we briefly evoked H^+-gated currents with the application of pH 6.0 extracellular solutions for 5 s. We then returned the pH to 7.4 and continued to measure postsynaptic currents every 10 s for several minutes (Fig. 4). Peak amplitudes of AMPAR, NMDAR, and $GABA_AR$ postsynaptic currents were unchanged following acid application (Fig. 4, *A–C*, $n = 4–5$). AMPAR EPSCs were increased robustly when we applied 2 μM 4-β-phorbol-12,13-dibutyrate (PDBu), a diacylglycerol analog that potentiates synaptic transmission through protein kinase C and other mechanisms (Wierda et al. 2007) (Fig. 4*D*, $n = 6$). This indicates that our experimental configuration could support signal transduction–dependent changes in synaptic transmission. To further conserve intracellular signaling mechanisms, we performed the same experiment using nystatin-based perforated-patch recording. Again, we did

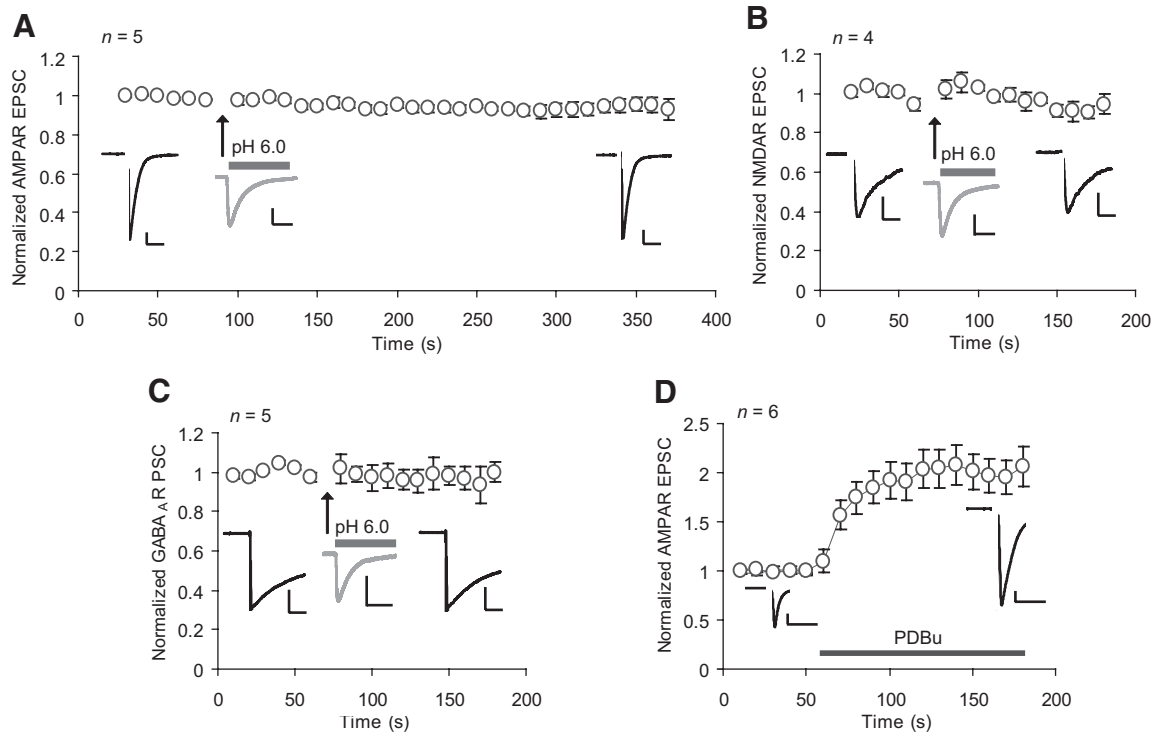

FIG. 4. The effects of acute ASIC activation by exogenously applied acid on postsynaptic currents. *A–C*: time courses of the changes of AMPAR EPSC (*A*), NMDAR EPSC (*B*), and $GABA_A$R PSC (*C*) following ASIC activation in wild-type autaptic neurons. Postsynaptic currents with stable peak amplitudes were recorded before and after a 6- to 7-s application of pH 6.0 extracellular solution (arrows and gray bars), which induced typical H^+-gated currents in wild-type neurons (*inset*, *gray traces*). Postsynaptic currents were normalized to the currents preceding the acid application. Representative traces of postsynaptic currents before and after acid application are shown (*inset*, *black traces*). Scale bars: 0.5 nA/50 ms for postsynaptic currents; 0.5 nA/2 s for H^+-gated currents. *D*: the effect of 4-β-phorbol-12,13-dibutyrate (PDBu), a diacylglycerol analog on AMPAR EPSC. PDBu (2 μM) was applied continuously for 2 min as indicated by the black bar in the graph. AMPAR EPSCs were normalized to the EPSCs preceding PDBu application. AMPAR EPSC traces before and during PDBu application are shown (*inset*). Scale bars: 0.5 nA and 50 ms.

not observe changes in postsynaptic current amplitudes following acid application ($n = 4$–5; data not shown). These results suggest that acute activation of ASICs does not rapidly alter postsynaptic currents.

Paired-pulse ratio is reduced in ASIC1 knockout neurons

Our results suggest that the decrease in the AMPAR/NMDAR EPSC ratio in ASIC1 knockout neurons is not due to activation of postsynaptic ASIC currents during the recording interval. To determine whether other aspects of synaptic transmission are altered in ASIC knockout neurons, we assessed the synaptic response to repetitive and paired-pulse stimulation (Mennerick and Zorumski 1995). A pair of stimuli with short intervals from 20 to 400 ms was applied, and the paired-pulse ratio (PPR) was determined by dividing the peak amplitude of the second AMPAR EPSC by the peak amplitude of the first EPSC (Fig. 5*A*). Compared with wild-type neurons, the PPRs with interpulse intervals of 50, 100, and 200 ms were significantly reduced in ASIC1 knockout neurons (Fig. 5, *A* and *B*, $P < 0.05$, wild-type vs. ASIC1 knockout, one-way ANOVA). Furthermore, during a short train of repetitive stimuli with 50-ms intervals, the amplitudes of the second through the fifth AMPAR EPSCs normalized to the first EPSC amplitude were reduced in ASIC1 knockout neurons compared with wild-type neurons (Fig. 5, *C* and *D*).

The fact that the PPR was altered was particularly surprising. Previous studies analyzing extracellular field potentials of Schaffer collateral–CA1 synapses in hippocampal slices did not observe changes in paired-pulse facilitation between ASIC1 knockout and wild-type mice. In contrast, we found that the PPR of ASIC1 knockout neurons in microisland cultures was reduced. The reason for this discrepancy is unclear. However, more variables such as polysynaptic activity contribute to the PPR in hippocampal slices compared with the PPR in microisland cultures (Mennerick and Zorumski 1995), and the simplicity and enhanced experimental control over these variables in the microisland culture system may have facilitated the detection of alterations in PPR. However, we also tested whether our pH buffer conditions may have allowed observation of altered PPR. Our experiments use a lower HEPES concentration (0.8 mM) compared with others (10 mM) to facilitate ASIC activation by endogenous acidic fluctuations in pH. To determine whether the difference in PPR was due to the low concentration of pH buffer used in our studies, we analyzed postsynaptic currents and PPR when the external buffer was increased to 10 mM HEPES, a concentration of HEPES that supports a buffering capacity close to that of CO_2/bicarbonate and phosphate buffers in vivo (24 mM HCO_3^- and 1 mM $H_2PO_4^-$ under 5% CO_2). We found that increasing the concentration of HEPES from 0.8 to 10 mM slightly reduced the peak amplitude of AMPAR EPSCs, NMDAR EPSCs, and $GABA_A$R PSCs. However, this effect was not different between wild-type, ASIC1 knockout, and ASIC2 knockout neurons (Fig. 6, *A* and *B*, $n = 6$–24, $P = 0.48$, 0.83, and 0.60 for

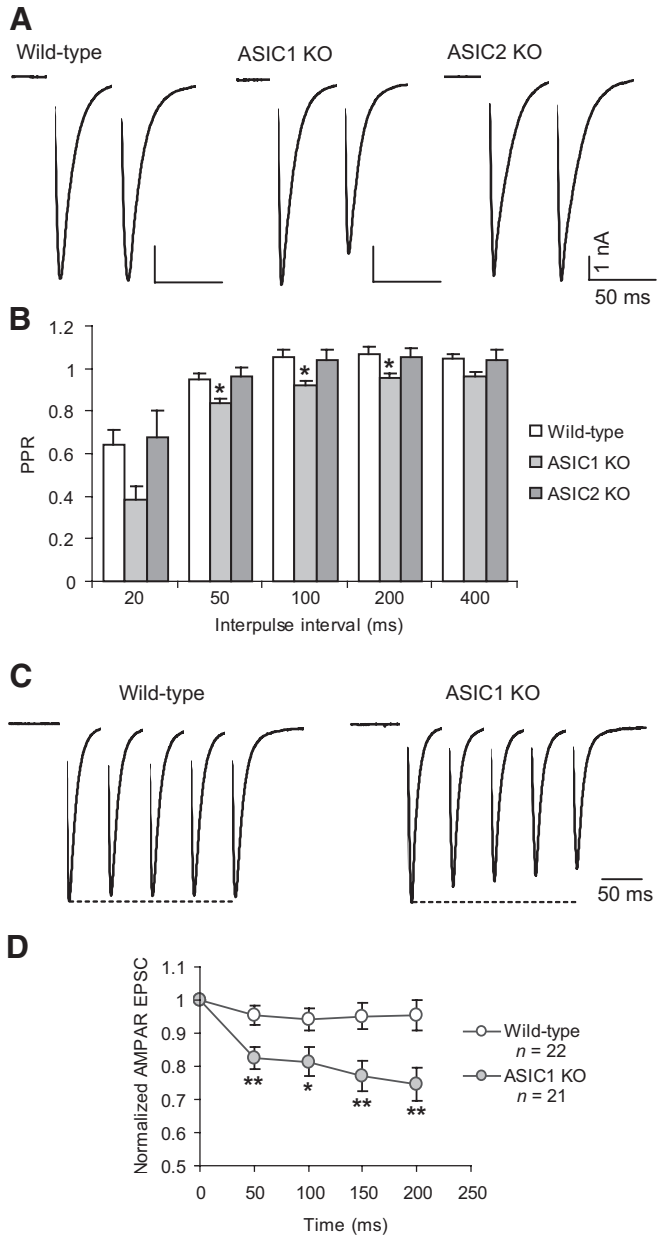

FIG. 5. Paired-pulse ratio (PPR) and AMPAR EPSCs during short trains of repetitive stimuli in autaptic neurons. *A*: representative traces of AMPAR EPSCs evoked by paired pulse in wild-type, ASIC1 knockout, and ASIC2 knockout neurons. Glutamatergic autaptic neurons were stimulated with a pair of stimuli with 50-ms interval in the presence of 2 mM Ca^{2+} and 1 mM Mg^{2+}. *B*: quantification of PPR at intervals from 20 to 400 ms in wild-type, ASIC1 knockout, and ASIC2 knockout neurons. PPR was calculated as the ratio of the peak amplitude of the second AMPAR EPSC to the peak amplitude of the first AMPAR EPSC. $n = 11$–58 for wild-type, $n = 7$–29 for ASIC1 knockout, and $n = 6$–10 for ASIC2 knockout neurons. $^*P < 0.05$, wild-type vs. ASIC1 knockout neurons, one-way ANOVA. *C*: representative trace of AMPAR EPSCs evoked by 5 successive stimuli with 50-ms interval in the presence of 2 mM Ca^{2+} and 1 mM Mg^{2+} in wild-type and ASIC1 knockout neurons. *D*: quantification of AMPAR EPSCs during a short train of 5 repetitive stimuli in wild-type and ASIC1 knockout neurons. $^*P < 0.05$, $^{**}P < 0.01$, unpaired *t*-test.

AMPAR EPSC, NMDAR EPSC, and $GABA_AR$ PSC, respectively, one-way ANOVA). Furthermore, PPR with 50-ms interval was not significantly altered by increasing HEPES concentration from 0.8 to 10 mM in wild-type neurons (Fig. 6, *C* and *D*, $n = 15$, $P = 0.81$, paired *t*-test). This indicates that the difference in the PPR between wild-type and ASIC1 knockout neurons is not due to the low concentration of pH buffer (0.8 mM HEPES).

We also analyzed whether the reduction in the PPR was due to the loss of ASIC currents within the second EPSC. To test this, we measured residual currents in the presence of CNQX and AP5 in a paired-pulse protocol with a 50-ms interval (Fig. 6*E*). We did not observe a significant difference in the relative contribution of residual current to peak amplitude of AMPAR EPSC between the first and the second stimulation in either wild-type or ASIC1 knockout neurons (Fig. 6*F*, residual current after the first and the second stimulation = 4.7 ± 0.8 and 4.7 ± 0.6% of peak AMPAR EPSC, $n = 5$, $P = 0.94$ for wild-type; 5.5 ± 5.8 and 5.8 ± 0.78%, $n = 4$, $P = 0.73$ for ASIC1 knockout, paired *t*-test). Furthermore, inhibition of ASICs with amiloride did not affect the PPR with a 50-ms interval in either wild-type or ASIC1 knockout neurons (Fig. 6, *G* and *H*, 102 ± 2.6% of pre-amiloride control, $n = 4$, $P = 0.51$ for wild-type; 95 ± 2.7%, $n = 4$, $P = 0.17$ for ASIC1 knockout, paired *t*-test). These results suggest that the difference in PPR between wild-type and ASIC1 knockout neurons is not due to the direct contribution of ASIC current to AMPAR EPSC.

Frequency of spontaneous neurotransmitter release is increased in ASIC1 knockout neurons

Alterations in the PPR can be due to multiple factors. To further define the synaptic alterations in ASIC1 knockout neurons, we performed quantal analyses on spontaneous miniature (m) EPSCs of wild-type and ASIC1 knockout neurons in conventional mass culture (Mennerick et al. 1995). We recorded AMPAR-mediated mEPSC in extracellular solution containing 1 mM Mg^{2+}, 30 μM bicuculline, and 1 μM tetrodotoxin to prevent action potential firing (Fig. 7*A*). The average peak amplitude of mEPSC was not different between wild-type and ASIC1 knockout neurons (Fig. 7*B*, 19.8 ± 2.2 pA, $n = 11$ neurons for wild-type, 21.1 ± 2.5 pA, $n = 8$ neurons for ASIC1 knockout, $P = 0.70$, unpaired *t*-test). In addition, neither the decay time constant nor the charge transfer of mEPSCs was different between wild-type and ASIC1 knockout neurons (decay time constant of mEPSC = 6.9 ± 0.1 and 7.1 ± 0.1 ms, for wild-type and ASIC1 knockout, $P = 0.10$, unpaired *t*-test; charge transfer of mEPSC = 102 ± 11 and 105 ± 12 fC for wild-type and ASIC1 knockout, $P = 0.86$, unpaired *t*-test). These results indicate that the postsynaptic response to spontaneous fusion of a single synaptic vesicle is not different in ASIC1 knockout neurons. However, mEPSCs were more frequent in ASIC1 knockout neurons than in wild-type neurons (Fig. 7*C*, 2.3 ± 0.2 Hz for wild-type; 5.1 ± 1.1 Hz for ASIC1 knockout, $P < 0.05$, unpaired *t*-test). An increase in mEPSC frequency is commonly caused by an increase in the total number of synapses, an increase in the size of the readily releasable pool (RRP) of synaptic vesicles, or an increase in the probability of neurotransmitter release. Previous studies have determined that the density of dendritic spines is equivalent in ASIC1 knockout and wild-type neurons in hippocampal slices (Zha et al. 2006). This suggests that the increased frequency of mEPSCs may be due to a larger number

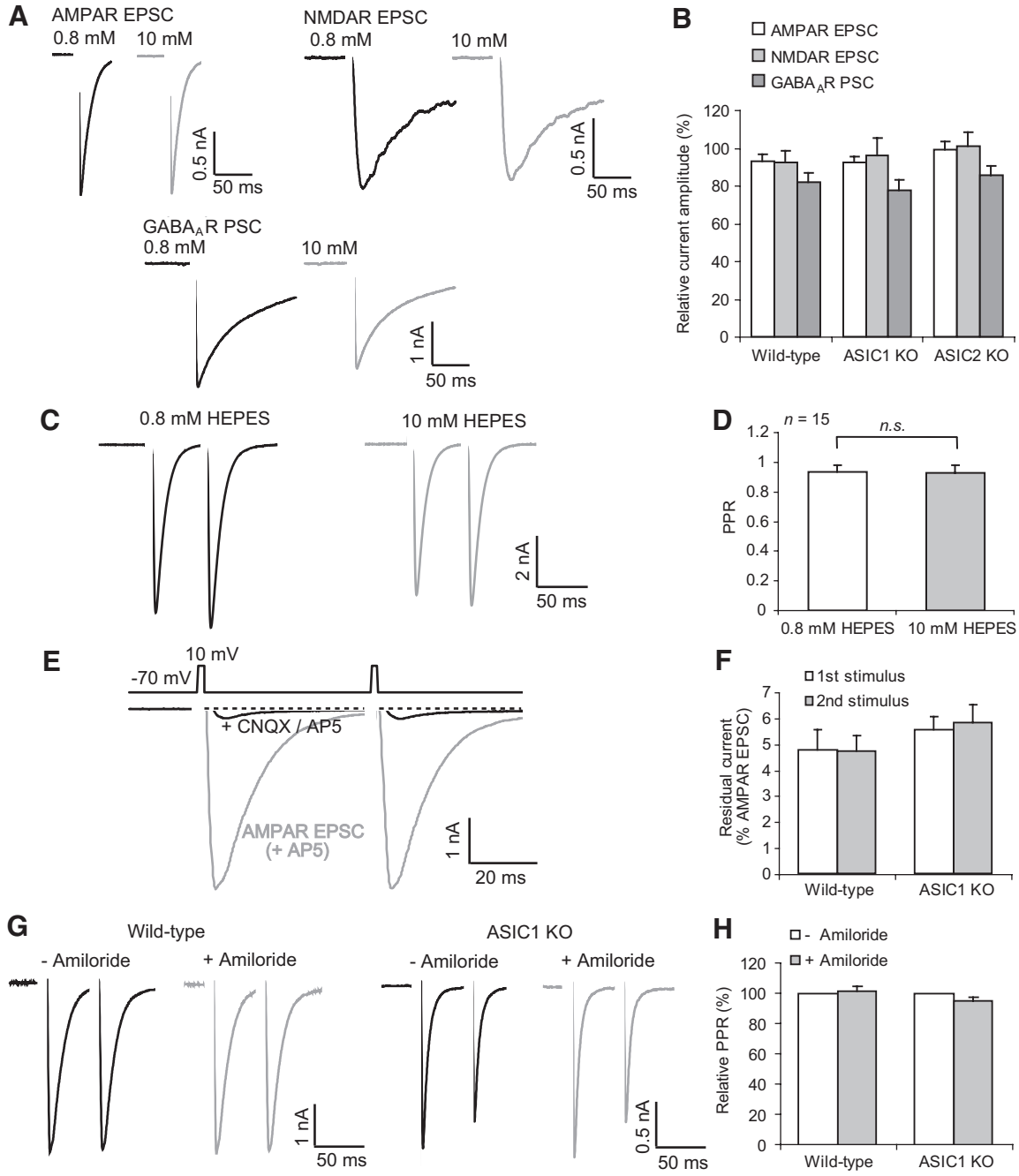

FIG. 6. The effects of HEPES concentration and amiloride on AP-evoked postsynaptic currents and the PPR. *A*: representative traces of AMPAR EPSC, NMDAR EPSC, and GABA$_A$R PSC from wild-type neurons. Postsynaptic currents were recorded from the same autaptic neuron in 0.8 mM (*black trace*) and 10 mM (*gray trace*) HEPES-containing extracellular solutions. *B*: the effect of the HEPES concentration on postsynaptic currents. Postsynaptic currents were recorded in 0.8 mM and 10 mM HEPES-containing extracellular solutions from wild-type, ASIC1 knockout, or ASIC2 knockout neurons. Within each neuron, current amplitude in 10 mM HEPES solution was normalized to that in 0.8 mM HEPES solution. These relative current amplitudes (%) were not significantly different between wild-type, ASIC1 knockout, and ASIC2 knockout neurons ($n = 6$–24, $P = 0.48$, 0.83, and 0.60 for AMPAR EPSC, NMDAR EPSC, and GABA$_A$R PSC, respectively; one-way ANOVA). *C*: representative traces of AMPAR EPSC in a wild-type neuron evoked by the paired-pulse protocol of 50-ms interval in the extracellular solution containing 2 mM Ca^{2+} and 1 mM Mg^{2+} with 0.8 mM (*black trace*) and 10 mM (*gray trace*) HEPES. *D*: quantification of the effect of the HEPES concentration on the PPR. The PPR was not significantly different between 0.8 and 10 mM HEPES ($n = 15$, $P = 0.81$, paired *t*-test). *E*: representative traces of AMPAR EPSC and residual current in the presence of CNQX and AP5 in a wild-type autaptic neuron. AMPAR EPSC was recorded in the presence of AP5 (*gray trace*), and residual current was isolated using CNQX and AP5 (*black trace*). Voltage steps above the traces indicate transient membrane depolarization from −70 to 10 mV used to evoke APs with 50-ms interval. *F*: quantification of the ratio of the residual current in the presence of CNQX and AP5 to peak AMPAR EPSC in wild-type ($n = 5$) and ASIC1 knockout ($n = 4$) neurons. There is no significant difference in the contribution of residual current to peak AMPAR EPSC between the first and the second stimulation in either a wild-type or an ASIC1 knockout neuron ($n = 5$, $P = 0.94$ for wild-type; $n = 4$, $P = 0.73$ for ASIC1 knockout, paired *t*-test). *G*: representative traces of AMPAR EPSC evoked by the paired-pulse protocol of 50-ms interval before (−amiloride, *black trace*) and during 300 μM amiloride application (+amiloride, *gray trace*) in wild-type and ASIC1 knockout neurons. *H*: quantification of the effect of the amiloride on PPR. PPR during amiloride application (+amiloride) was normalized to PPR before amiloride treatment (−amiloride). Amiloride did not change PPR significantly in either wild-type or ASIC1 knockout neurons ($n = 4$, $P = 0.51$ for wild-type; $n = 4$, $P = 0.17$ for ASIC1 knockout, paired *t*-test).

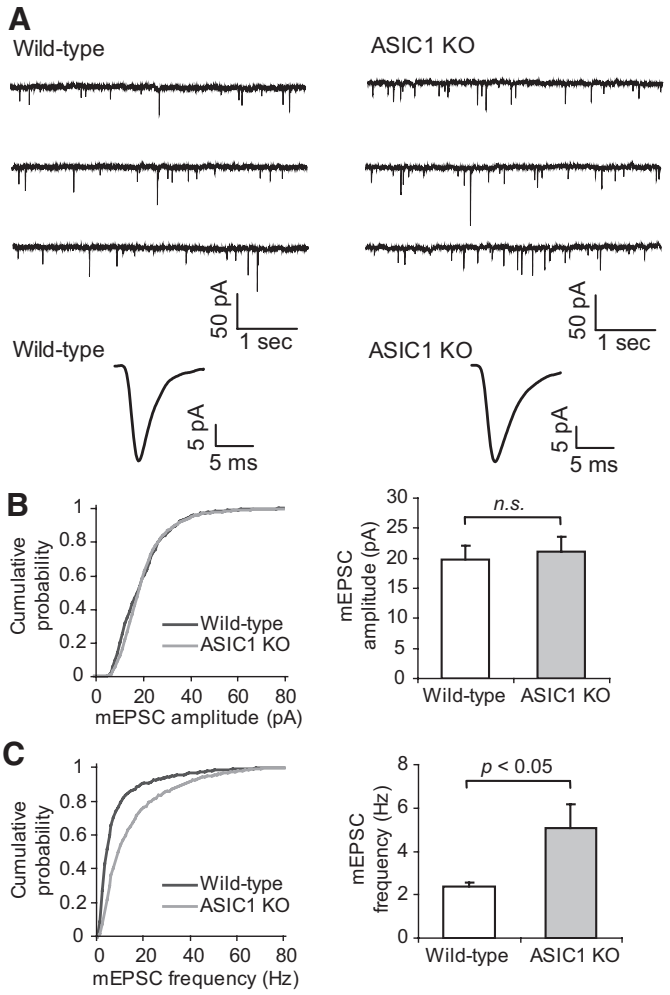

FIG. 7. Quantal analyses of AMPAR-mediated miniature EPSC (mEPSC) of hippocampal neurons in mass culture. *A*: representative traces of mEPSC in wild-type (*left*) and ASIC1 knockout (*right*) neurons in mass culture. AMPAR-mediated mEPSC was recorded in extracellular solution containing 1 mM Mg^{2+}, 30 μM bicuculline, and 1 μM tetrodotoxin. Averaged mEPSCs in the same wild-type and ASIC1 knockout neurons are also shown (*bottom traces*). *B*: cumulative histogram of peak amplitude of mEPSC from 1,179 and 2,399 events from 11 wild-type and 8 ASIC1 knockout neurons respectively (*left*). Average peak amplitude of mEPSC was calculated in each neuron and quantified as a bar graph (*right*, mean ± SE). *C*: cumulative histogram of instantaneous frequency of mEPSC (*left*). Average frequency of mEPSC was calculated in each neuron and quantified as bar graph (*right*). Statistical significance was assessed using unpaired *t*-test.

of synaptic vesicles in the RRP or a higher probability of neurotransmitter release in ASIC1 knockout neurons.

RRP size and refilling are not different in ASIC1 knockout neurons

The RRP size and refilling were analyzed using hypertonic sucrose solution. When hypertonic sucrose is applied, synaptic vesicles in the entire RRP release neurotransmitters in a Ca^{2+}-independent manner and produce postsynaptic currents proportional to the size of the RRP (Rosenmund and Stevens 1996). Extracellular solution containing 500 mM sucrose was applied to neurons in mass culture for 4–5 s and the sucrose-induced postsynaptic current response was recorded in 1 mM Mg^{2+}, 30 μM bicuculline, and 1 μM tetrodotoxin (Fig. 8*A*). This sucrose-induced response was completely inhibited by 10 μM CNQX (Fig. 8*A*), indicating that it was mediated by AMPARs (Rosenmund and Stevens 1996). RRP size was estimated from the sucrose-induced charge transfer calculated by integrating the transient component of the sucrose-evoked current. We determined that the RRP size was not significantly different between wild-type and ASIC1 knockout neurons (Fig. 8*B*, 0.86 ± 0.09 nC, $n = 20$ for wild-type, 0.95 ± 0.11 nC, $n = 24$ for ASIC1 knockout, $P = 0.52$, unpaired *t*-test). The RRP refilling was also analyzed by comparing the charge transfer in response to a second sucrose application 3–4 s after the first (Fig. 8*A*) (Priller et al. 2006). RRP refilling, estimated as the ratio of the charge transfer by the second sucrose application to the charge transfer induced by the first sucrose application, was not significantly different between wild-type and ASIC1 knockout neurons (Fig. 8*C*, 0.53 ± 0.02, $n = 17$ for wild-type, 0.52 ± 0.03, $n = 20$ for ASIC1 knockout, $P = 0.93$, unpaired *t*-test). These results indicate that the size and refilling of the RRP are not different between wild-type and ASIC1 knockout neurons in conventional mass culture.

Progressive block of NMDARs by MK-801 was faster in ASIC1 knockout neurons

An increase in the release probability could account for both the more frequent mEPSCs and the reduced PPR observed in ASIC1 knockout neurons (Zucker and Regehr 2002). The release probability of ASIC1 knockout neurons was analyzed using progressive block of the NMDARs by MK-801 (Rosenmund et al. 1993). Because MK-801 irreversibly blocks NMDARs while they are open, the rate of NMDAR EPSC decrease correlates with the probability of neurotransmitter release (Futai et al. 2007; Rosenmund et al. 1993). Thus the higher the release probability is, the faster the rate of MK-801–induced decrease of NMDAR EPSCs. The rate of progressive block of NMDAR by MK-801 could also be affected by the duration of NMDAR opening. Because NR2B-containing NMDARs open longer than NR2A-containing NMDARs, a difference in the ratio of NR2B- to NR2A-containing NMDARs can hamper interpretation of NMDAR progressive block by MK-801 (Monyer et al. 1992). However, we find that the weighted mean decay time constant of NMDAR EPSCs was not different between wild-type and ASIC1 knockout neurons (198 ± 14, $n = 45$ for wild-type, and 182 ± 9, $n = 48$ for ASIC1 knockout, $P = 0.37$, unpaired *t*-test), suggesting that NMDARs remain open for similar periods of time in response to glutamate.

Under normal conditions, the NMDAR EPSCs of autaptic neurons stimulated every 10 s did not change significantly over time (Fig. 9*A*). In the presence of 10 μM MK-801, the NMDAR EPSCs gradually decreased in a stimulus-dependent manner (Fig. 9*A*). NMDAR EPSC amplitudes were normalized to the first NMDAR EPSC in the presence of MK-801 and plotted against stimulus number. The data were fit to a single-exponential equation, and the rate of the decrease of the NMDAR EPSCs was quantified by calculating the tau (τ) in stimulus number (Fig. 9, *B–D*). The rate of NMDAR EPSC decrease in the presence of MK-801 was faster and the tau was significantly reduced in ASIC1 knockout neurons compared with wild-type neurons (Fig. 9, *C* and *D*, $\tau = 22.4 \pm 1.9$ stimuli, $n = 9$ for wild-type, 16.1 ± 1.5 stimuli, $n = 8$ for

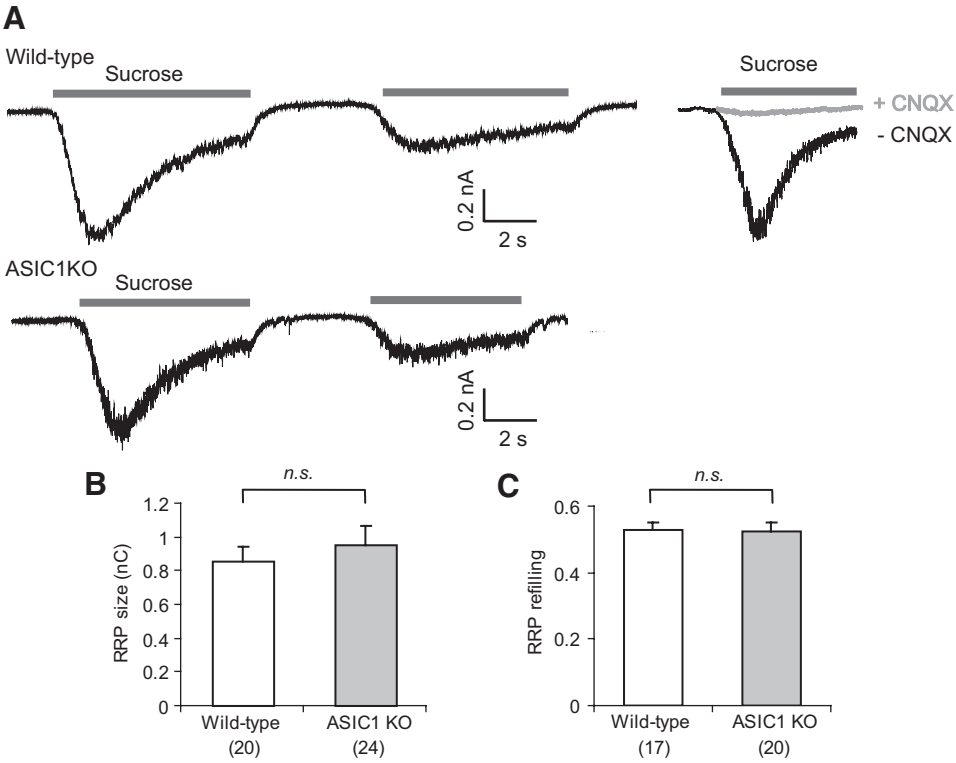

FIG. 8. Readily releasable pool (RRP) size and RRP refilling of wild-type and ASIC1 knockout neurons. *A*: representative recordings of sucrose response in wild-type (*top traces*) and ASIC1 knockout (*bottom trace*) neurons in mass culture. Hypertonic sucrose (500 mM) was applied for 4–5 s (gray bars), and the sucrose-induced current was recorded in extracellular solution containing 1 mM Mg^{2+}, 30 μM bicuculline, and 1 μM tetrodotoxin. The sucrose response was inhibited completely by 10 μM CNQX (+ CNQX, *top right trace*). *B*: total charge transfer by the application of hypertonic sucrose. RRP size was estimated from hypertonic sucrose-induced charge transfer calculated by integrating the transient component of the sucrose response curve. *C*: RRP refilling was estimated from analysis of a second sucrose response evoked 3–4 s after the first sucrose application. The ratio of the charge transfer by the second sucrose application to the charge transfer induced by the first sucrose application was calculated. Numbers in parentheses indicate the numbers of neurons examined. Statistical significance was assessed using unpaired *t*-test.

ASIC1 knockout, $P < 0.05$, unpaired *t*-test). These results suggest that the release probability is higher in ASIC1 knockout glutamatergic neurons.

Neurotransmitter release probability is increased in ASIC1 knockout neurons

A second experiment was used to assess the release probability of wild-type and ASIC knockout neurons. Both the AP-evoked EPSC and hypertonic sucrose-induced current were recorded in the same glutamatergic autaptic neurons (Fig. 10*A*). The probability of neurotransmitter release was calculated by dividing the charge transfer of AP-evoked EPSC by the charge transfer of the response induced by depletion of the RRP of synaptic vesicles with hypertonic sucrose (Molder et al. 2004; Rhee et al. 2002). The release probability of wild-type and ASIC2 knockout neurons was 6–7% (Fig. 10*D*, 7.0 ± 0.8%, $n = 27$ for wild-type, and 6.2 ± 0.5%, $n = 12$ for ASIC2 knockout), which is close to the value obtained in other studies (Rhee et al. 2002). The release probability of ASIC1 knockout neurons was significantly higher compared with wild-type and ASIC2 knockout neurons (Fig. 10*D*, 10.9 ± 1.7%, $n = 19$ for ASIC1 knockout, $P < 0.05$, ASIC1 knockout vs. wild-type or ASIC2 knockout, one-way ANOVA). Together, this experiment and the experiment assessing progressive block of NMDAR by MK-801 (Fig. 9) indicate that ASIC1 knockout neurons have a higher probability of neurotransmitter release than that of wild-type neurons.

Rescue of ASIC1 knockout neurons by ASIC1a expression

We find that the release probability is higher in neurons from ASIC1 knockout mice compared with neurons from wild-type mice. To determine whether this effect is the result of developmental compensation in response to ASIC1 gene disruption, we performed rescue experiments in cultured neurons. Hippocampal neurons from ASIC1 knockout mice were transfected during isolation with either vector alone or vector-expressing ASIC1a. Neurons were plated to foster microisland conditions, and whole cell patch clamping was used to measure acid-evoked currents and synaptic transmission after 14–20 days in culture. We found that extracellular acid (pH 6.0) failed to evoke H^+-gated currents in ASIC1 knockout neurons transfected with vector alone (Fig. 11*A*, peak amplitude = 74 ± 17 pA, $n = 9$). In ASIC1a-transfected ASIC1 knockout neurons, extracellular acid induced typical H^+-gated currents with characteristics similar to those of wild-type neurons (Fig. 11*A*, peak amplitude = 1,489 ± 458 pA, $n = 6$, $P < 0.05$, ASIC1a-transfected vs. vector-transfected neurons, unpaired *t*-test). Thus transfection of ASIC1 knockout neurons with ASIC1a restored H^+-gated currents. We next examined synaptic transmission in transfected ASIC1 knockout neurons. $GABA_A$R-mediated postsynaptic currents were not significantly different in ASIC1 knockout neurons transfected with ASIC1a or vector alone (peak amplitude = 5.5 ± 1.3 nA, $n = 6$ for ASIC1a-transfected neurons, and 3.5 ± 0.8 nA, $n = 8$ for vector-transfected neurons, $P = 0.23$, unpaired *t*-test). However, the peak amplitude of AMPAR-mediated EPSCs was profoundly smaller in ASIC1a-transfected neurons compared with vector-transfected neurons (Fig. 11*B*, 1.60 ± 0.27 nA, $n = 6$ for ASIC1a-transfected neurons, and 4.42 ± 0.66 nA, $n = 9$ for vector-transfected neurons, $P < 0.01$, unpaired *t*-test). Furthermore, the PPRs at interpulse intervals of 40 and 50 ms were increased in ASIC1a-transfected neurons (Fig. 11*C*, $P < 0.05$, unpaired *t*-test). Because the PPR is inversely correlated with release probability (Zucker and Regehr 2002), these results suggest that release probability of ASIC1 knockout neurons

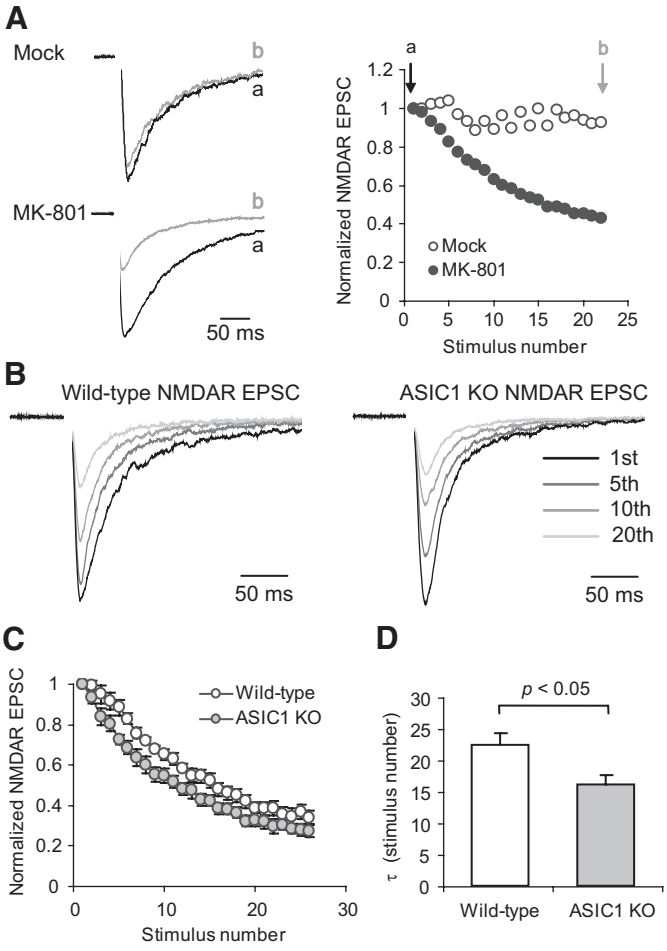

FIG. 9. The progressive block of NMDAR by MK-801 in glutamatergic autaptic neurons. *A*: representative traces of the first (*a*, black) and 22nd (*b*, gray) NMDAR EPSC (*left*), and the time course of NMDAR EPSC change (*right*) in the presence or absence of 10 μM MK-801 in a wild-type autaptic neuron. EPSCs were evoked in the presence of MK-801 or vehicle (mock) every 10 s for 4 min in Mg^{2+}-free solution with 10 μM CNQX. *B*: representative trace of NMDAR EPSCs (1st, 5th, 10th, and 20th) in the presence of MK-801 in wild-type (*left*) and ASIC1 knockout neurons (*right*). *C*: stimulus-dependent decrease of NMDAR EPSC by MK-801. Peak amplitudes of NMDAR EPSC were normalized to that of the first NMDAR EPSC in the presence of MK-801. $n = 8$ for wild-type; $n = 8$ for ASIC1 knockout neurons. *D*: quantification of the rate of the NMDAR EPSC decrease by MK-801. Tau (τ) in stimulus number was calculated by fitting the curve of NMDAR EPSC change to single-exponential equations, $I(n) = I_{1st} \exp(-n/\tau)$, where n is stimulus number, $I(n)$ is peak amplitude of nth NMDAR EPSC, and I_{1st} is the peak amplitude of the first NDMAR EPSC in the presence of MK-801. Statistical significance was assessed using an unpaired *t*-test.

transfected with ASIC1a is decreased. Moreover, we suggest that the decreased release probability also resulted in the smaller amplitude of AMPAR EPSCs in ASIC1a-transfected ASIC1 knockout neurons. These experiments show that the PPR of ASIC1 knockout neurons can be restored by in vitro expression of ASIC1a and suggest that the increase in release probability observed in ASIC1 knockout neurons is not due to developmental compensation.

DISCUSSION

Given that ASICs are activated by extracellular protons, a role for ASICs in biological processes involving extracellular acidosis is not surprising. For example, ASICs mediate acid-induced nociception during inflammation (Price et al. 2001; Sutherland et al. 2001). ASICs are involved in the retinal response to light where acidic pH changes are known to influence neuronal signaling (Ettaiche et al. 2004, 2006). In the brain, ASIC1a activation causes neuronal death during prolonged acidosis following ischemia (Xiong et al. 2004, 2006). However, ASICs are also involved in neuronal processes where the role of extracellular acidosis is not well defined. For example, ASIC1 is required for normal fear-related behaviors as well as learning and memory (Wemmie et al. 2002, 2003, 2004). Although rapid extracellular pH transients have been

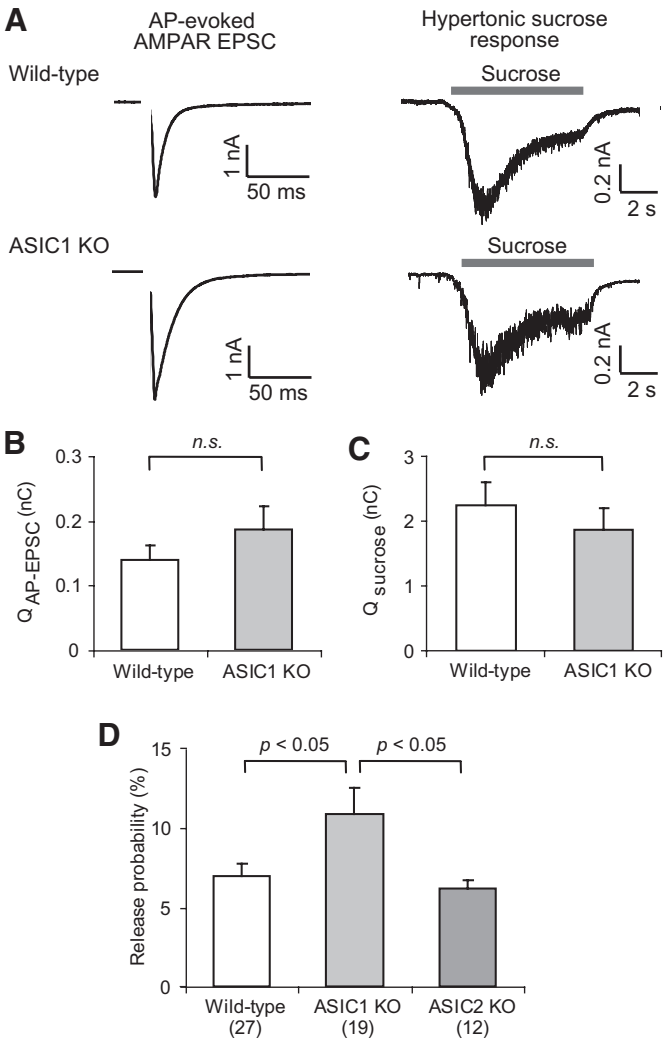

FIG. 10. Release probability measured in glutamatergic autaptic neurons on microislands. *A*: representative traces of AP-evoked AMPAR EPSC (*left*) and 500 mM sucrose-induced response (*right*) of wild-type (*top traces*) and ASIC1 knockout (*bottom traces*) neurons. Both AMPAR EPSC and sucrose response were recorded in the same neuron in the presence of 1 mM Mg^{2+}. *B* and *C*: quantification of AP-evoked (*B*) and sucrose-induced (*C*) charge transfers calculated by integrating AMPAR EPSC and hypertonic sucrose response curves. $n = 27$ for wild-type and $n = 19$ for ASIC1 knockout. *D*: quantification of the release probability of wild-type, ASIC1 knockout, and ASIC2 knockout neurons. The probability of neurotransmitter release was calculated by dividing total charge transfer of AP-evoked EPSC by hypertonic sucrose-induced charge transfer. Numbers in parentheses indicate the numbers of neurons examined. One-way ANOVA was used to determined statistical significance.

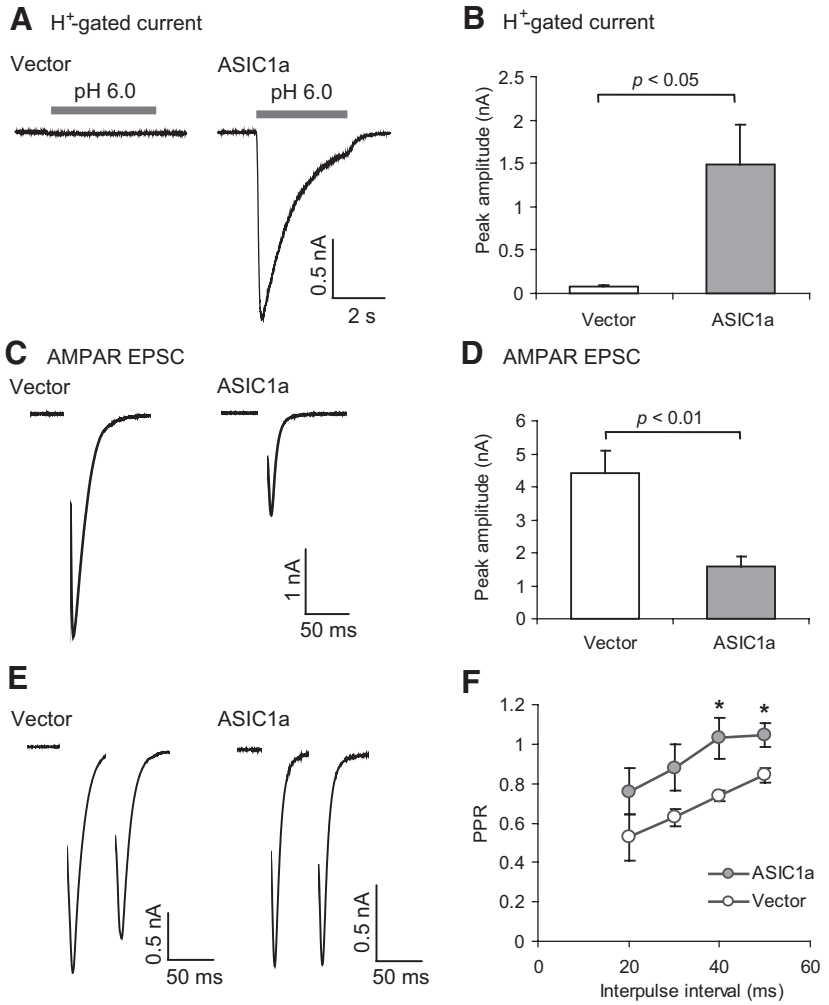

FIG. 11. Rescue of ASIC1 knockout neurons by ASIC1a expression. *A*: representative traces of H^+-gated currents in ASIC1 knockout neurons transfected with vector (pcDNA3.1, *left*) or human ASIC1a (*right*). To evoke H^+-gated currents, we exchanged the extracellular solution of pH 7.4 to pH 6.0 for 6–7 s (gray bars). *B*: peak amplitude of pH 6.0–induced H^+-gated currents. $n = 6$ for ASIC1a-transfected neurons; $n = 9$ for vector-transfected neurons; unpaired *t*-test. *C*: representative traces of whole cell AMPAR-mediated EPSC in ASIC1 knockout neurons transfected with vector or ASIC1a. AMPAR EPSCs were recorded in the presence of 1 mM Mg^{2+}, and membrane potential was held at −70 mV. *D*: peak amplitude of the AMPAR EPSCs. $n = 6$ for ASIC1a-transfected neurons; $n = 9$ for vector-transfected neurons; unpaired *t*-test. *E*: representative traces of AMPAR EPSCs evoked by a paired pulse with 50-ms interval in the presence of 2 mM Ca^{2+} and 1 mM Mg^{2+}. *F*: quantification of the PPR at intervals from 20 to 50 ms. The PPR was calculated as the ratio of the peak amplitude of the second AMPAR EPSC to the peak amplitude of the first AMPAR EPSC. $n = 4–6$ for ASIC1a-transfected neurons; $n = 5–9$ for vector-transfected neurons. $^*P < 0.05$, unpaired *t*-test. Single glutamatergic neurons on microisland were selected for recording H^+-gated currents and AMPAR EPSC in these experiments.

observed during synaptic transmission (Krishtal et al. 1987), how ASICs impact neurotransmission is not clear.

In this study, we investigated the role of ASICs in synaptic transmission by comparing postsynaptic currents of cultured hippocampal neurons from wild-type and both ASIC1 and ASIC2 knockout mice. We observed alterations in synaptic transmission in glutamatergic neurons from ASIC1 knockout mice using multiple experimental paradigms. First, the AMPAR/NMDAR EPSC ratio was reduced in ASIC1 knockout neurons (Fig. 2*F*). Second, the paired-pulse ratio (PPR) of AMPAR EPSC was reduced and the depression of AMPAR EPSCs during a short train of stimuli was greater in ASIC1 knockout neurons (Fig. 5). Alterations in the PPR can be due to both presynaptic and postsynaptic mechanisms. In an effort to identify the nature of the PPR changes in ASIC1 knockout neurons, we assessed other aspects of synaptic transmission. We determined that the quantal size of mEPSCs, the size of readily releasable pool (RRP) of synaptic vesicles, and RRP refilling were not significantly different in ASIC1 knockout neurons compared with wild-type neurons (Figs. 7 and 8). In contrast, the frequency of mEPSCs was increased (Fig. 7*C*), and the progressive block of NMDAR by MK-801 was faster in ASIC1 knockout neurons (Fig. 9). These results suggest that the reduced PPR in ASIC1 knockout neurons is due to the increased probability of neurotransmitter release. This was confirmed by the observation that the release probability, as measured by the ratio of AP-evoked to hypertonic sucrose-evoked charge transfer, was increased in ASIC1 knockout neurons (Fig. 10). Together, these results support the conclusion that cultured ASIC1 knockout neurons have a higher release probability than that of wild-type neurons. Further, that mEPSC frequency increased and the release probability was augmented without a change in the RRP size suggest an enhanced fusion propensity of individual vesicles in ASIC1 knockout neurons. Transfection of ASIC1a increased the PPR of ASIC1 knockout neurons and reduced AMPAR EPSCs (Fig. 11). These results are consistent with an ASIC1a-dependent rescue of the release probability of ASIC1 knockout neurons and suggest that the increased release probability observed in ASIC1 knockout neurons is not likely due to developmental compensation. Interestingly, there were no significant differences in synaptic transmission in ASIC2 knockout neurons (Figs. 2*F*, 5*B*, and 10*D*), indicating that these alterations are specific to disruption of ASIC1.

Because the release probability is increased in ASIC1 knockout neurons, AP-evoked whole cell postsynaptic currents should be larger compared with wild-type neurons. Although the average peak amplitudes of single AP-evoked AMPAR EPSCs or NMDAR EPSCs were larger in ASIC1 knockout neurons (Figs. 2, *D* and *E* and 10*B*), the difference did not reach statistical significance, and we expect a greater increase in EPSC amplitude with such an increase in release probability.

We suggest that the postsynaptic response of ASIC1 knockout neurons is altered such that the EPSC amplitude is unchanged even with the increased release probability. In support of this idea, we did observe that AMPAR/NMDAR EPSC ratio was reduced in ASIC1 knockout neurons (Fig. 2*F*). Because the quantal size of AMPAR-mediated mEPSC was not changed in ASIC1 knockout neurons (Fig. 7*B*), it is not likely that the number of AMPARs per synapse or the conductance of individual postsynaptic AMPARs was different in the ASIC1 knockout neurons. In contrast, disruption of ASIC1 may have affected the ratio of AMPAR-expressing functional synapses to silent synapses that contain NMDAR but not AMPAR. Thus the number of AMPAR-expressing functional synapses may be reduced in ASIC1 knockout neurons. Such a reduction would mask the effect of enhanced release probability on AMPAR EPSCs. In rescue experiments, we did observe alterations in postsynaptic current consistent with altered release probability. ASIC1 knockout neurons transfected with ASIC1a displayed dramatically reduced AMPAR EPSCs compared with vector-transfected neurons, consistent with a decrease in release probability (Fig. 11*B*). This result suggests that presynaptic alterations in ASIC1 knockout neurons can be rescued by expression of ASIC1a in culture.

It is hypothesized that postsynaptic ASICs are activated by protons released from synaptic vesicles during neurotransmission. ASIC activation, in turn, contributes to depolarization and calcium-induced signaling cascades. This model has been difficult to prove and, like others before, we did not detect ASIC-mediated postsynaptic currents during synaptic transmission (Fig. 3, *A–D*). Even multiple stimulations failed to induce measurable ASIC-dependent currents (Fig. 6, *E* and *F*). Furthermore, we did not observe any ASIC-dependent effect of amiloride on AMPAR EPSC or PPR (Figs. 3, *E* and *F* and 6, *G* and *H*). Given the large postsynaptic currents recorded, the sensitivity of the method, and the presence of H^+-gated currents evoked by exogenous acid application in these neurons, we conclude that specific conditions must exist for ASICs to be activated in this manner and make a substantial contribution to the postsynaptic currents. However, definitive changes in synaptic transmission were observed in ASIC1 knockout neurons, even though ASIC currents were not detected during synaptic transmission. Our data suggest that the higher release probability in ASIC1 knockout neurons is due to either *1*) disruption of ASIC1a-specific signaling, which has long-term effects on presynaptic mechanisms, or *2*) loss of an unconventional nonionotropic ASIC function, which is not dependent on ion conduction of ASIC1a.

First, disruption of ASIC1a-specific signaling could have long-term effects on presynaptic mechanisms. Under normal conditions, ASIC1a activation could lead to long-term changes in synaptic transmission through activation of signal transduction cascades. ASIC1a homomultimers are Ca^{2+} permeable (Yermolaieva et al. 2004) and may activate Ca^{2+}/calmodulin-dependent protein kinase II (CaMKII). Phosphorylated CaMKIIα is reduced in brains from ASIC1 knockout mice (Zha et al. 2006), indicating that disruption of ASIC1 can influence the activation status of CaMKII, which is essential for the recruitment of AMPAR to synapses and for the LTP induction in the CA1 region of hippocampus (Lisman et al. 2002). CaMKII may also affect presynaptic mechanisms to alter neurotransmitter release (Chi et al. 2001; Llinás et al. 1991; Sanhueza et al. 2007; Waxham et al. 1993). To investigate the possibility that previous activation of ASIC1a causes changes in synaptic transmission, we assessed postsynaptic current following activation of ASICs by exogenous acid application. However, we did not observe changes in postsynaptic currents in the time frame assessed (2–5 min, Fig. 4). Thus ASIC1a-induced changes in signal transduction may occur under other specific conditions or require a longer period of time to manifest.

Second, changes in synaptic transmission of ASIC1 knockout neurons could be due to the loss of an unconventional nonionotropic ASIC function. Such "nonconducting" functions have been reported for other ion channels such as NMDARs (Alvarez et al. 2007) and HCN (I_h) channels (Beaumont and Zucker 2000; Beaumont et al. 2002; Zhong et al. 2004). ASIC1a could regulate release probability by direct interaction with neurotransmitter release machinery. Previous studies indicate that ASICs are localized postsynaptically (Wemmie et al. 2002; Zha et al. 2006), but do not exclude the possibility of ASIC1a at presynaptic sites (Alvarez de la Rosa et al. 2003). Ionotropic neurotransmitter receptors such as NMDA receptor, kainite receptor, and $GABA_A$ receptor are expressed both presynaptically and postsynaptically and regulate neurotransmitter release (MacDermott et al. 1999). Furthermore, ASIC1a, ASIC2a, and γ-ENaC form heteromeric channels in malignant glioma cells, and this complex interacts with syntaxin 1A, a component of the SNARE complex involved in exocytosis of synaptic vesicles (Berdiev et al. 2003). Although it is not known whether this interaction also occurs in neurons, this raises a possibility that ASICs might directly regulate neurotransmitter release. Alternatively, postsynaptic ASIC1a could affect synaptic transmission in a retrograde manner like postsynaptic PSD-95, which regulates neurotransmitter release by physical interaction with presynaptic neurexin (Futai et al. 2007). ASICs have a large extracellular loop of largely unknown function, and the extracellular loop of postsynaptic ASIC1a could physically interact with a presynaptic counterpart to directly regulate neurotransmitter release.

ASIC1 knockout mice exhibited defects in multiple aspects of learning and memory such as spatial learning, fear conditioning, and eye-blink conditioning (Wemmie et al. 2002, 2003). This suggests a fundamental role of ASIC1a in synaptic transmission and plasticity. Our results indicate that disruption of ASIC1 increases presynaptic neurotransmitter release. In the brain, the greater basal release probability might prevent additional increases in synaptic transmission and thus limit long-term potentiation in ASIC1 knockout mice (Wemmie et al. 2002). We observed altered paired-pulse modulation and depression during short trains of stimulation in ASIC1 knockout neurons. These types of short-term plasticity are important for information processing in neural networks (e.g., producing reliable response to repetitive activation) and contribute to normal behavior (Blitz et al. 2004). Thus dysregulation of short-term plasticity may also cause defects in multiple aspects of cognitive function in ASIC1 knockout mice. Our results indicate that the consequences of ASIC1 disruption are complex and influence both presynaptic and postsynaptic mechanisms. In addition, ASIC1a may play a fundamental role in synaptic transmission by regulating presynaptic release probability.

ACKNOWLEDGMENTS

We thank S. Mennerick (Washington University School of Medicine) for assistance with the microisland culture method as well as helpful discussions regarding the interpretation and design of experiments; J. Wemmie, M. Welsh, and M. Price (University of Iowa) for providing the ASIC1 and ASIC2 knockout mice; and D. Saffen, S. Mangel, and T. Sherwood (The Ohio State University) for thoughtful review of the manuscript.

GRANTS

This work was supported by National Science Foundation Grant IBN-0416920 to C. Askwith.

REFERENCES

Alvarez VA, Ridenour DA, Sabatini BL. Distinct structural and ionotropic roles of NMDA receptors in controlling spine and synapse stability. *J Neurosci* 27: 7365–7376, 2007.

Alvarez de la Rosa D, Krueger SR, Kolar A, Shao D, Fitzsimonds RM, Canessa CM. Distribution, subcellular localization and ontogeny of ASIC1 in the mammalian central nervous system. *J Physiol* 546: 77–87, 2003.

Askwith CC, Wemmie JA, Price MP, Rokhlina T, Welsh MJ. Acid-sensing ion channel 2 (ASIC2) modulates ASIC1 H+-activated currents in hippocampal neurons. *J Biol Chem* 279: 18296–18305, 2004.

Bassilana F, Champigny G, Waldmann R, de Weille JR, Heurteaux C, Lazdunski M. The acid-sensitive ionic channel subunit ASIC and the mammalian degenerin MDEG form a heteromultimeric H+-gated Na^+ channel with novel properties. *J Biol Chem* 272: 28819–28822, 1997.

Beaumont V, Zhong N, Froemke RC, Ball RW, Zucker RS. Temporal synaptic tagging by I(h) activation and actin: involvement in long-term facilitation and cAMP-induced synaptic enhancement. *Neuron* 33: 601–613, 2002.

Beaumont V, Zucker RS. Enhancement of synaptic transmission by cyclic AMP modulation of presynaptic Ih channels. *Nat Neurosci* 3: 133–141, 2000.

Bekkers JM, Stevens CF. Excitatory and inhibitory autaptic currents in isolated hippocampal neurons maintained in cell culture. *Proc Natl Acad Sci USA* 88: 7834–7838, 1991.

Benson CJ, Xie J, Wemmie JA, Price MP, Henss JM, Welsh MJ, Snyder PM. Heteromultimers of DEG/ENaC subunits form H+-gated channels in mouse sensory neurons. *Proc Natl Acad Sci USA* 99: 2338–2343, 2002.

Berdiev BK, Xia J, McLean LA, Markert JM, Gillespie GY, Mapstone TB, Naren AP, Jovov B, Bubien JK, Ji HL, Fuller CM, Kirk KL, Benos DJ. Acid-sensing ion channels in malignant gliomas. *J Biol Chem* 278: 15023–15034, 2003.

Blitz DM, Foster KA, Regehr WG. Short-term synaptic plasticity: a comparison of two synapses. *Nat Rev Neurosci* 5: 630–640, 2004.

Chavis P, Westbrook G. Integrins mediate functional pre- and postsynaptic maturation at a hippocampal synapse. *Nature* 411: 317–321, 2001.

Chi P, Greengard P, Ryan TA. Synapsin dispersion and reclustering during synaptic activity. *Nat Neurosci* 4: 1187–1193, 2001.

Cho JH, Askwith CC. Potentiation of acid-sensing ion channels by sulfhydryl compounds. *Am J Physiol Cell Physiol* 292: C2161–C2174, 2007.

DeVries SH. Exocytosed protons feedback to suppress the Ca^{2+} current in mammalian cone photoreceptors. *Neuron* 32: 1107–1117, 2001.

Ettaiche M, Deval E, Cougnon M, Lazdunski M, Voilley N. Silencing acid-sensing ion channel 1a alters cone-mediated retinal function. *J Neurosci* 26: 5800–5809, 2006.

Ettaiche M, Guy N, Hofman P, Lazdunski M, Waldmann R. Acid-sensing ion channel 2 is important for retinal function and protects against light-induced retinal degeneration. *J Neurosci* 24: 1005–1012, 2004.

Futai K, Kim MJ, Hashikawa T, Scheiffele P, Sheng M, Hayashi Y. Retrograde modulation of presynaptic release probability through signaling mediated by PSD-95-neuroligin. *Nat Neurosci* 10: 186–195, 2007.

Gao Y, Liu SS, Qiu S, Cheng W, Zheng J, Luo JH. Fluorescence resonance energy transfer analysis of subunit assembly of the ASIC channel. *Biochem Biophys Res Commun* 359: 143–150, 2007.

Garcia-Anoveros J, Derfler B, Neville-Golden J, Hyman BT, Corey DP. BNaC1 and BNaC2 constitute a new family of human neuronal sodium channels related to degenerins and epithelial sodium channels. *Proc Natl Acad Sci USA* 94: 1459–1464, 1997.

Hesselager M, Timmermann DB, Ahring PK. pH Dependency and desensitization kinetics of heterologously expressed combinations of acid-sensing ion channel subunits. *J Biol Chem* 279: 11006–11015, 2004.

Hosoi N, Arai I, Tachibana M. Group III metabotropic glutamate receptors and exocytosed protons inhibit L-type calcium currents in cones but not in rods. *J Neurosci* 25: 4062–4072, 2005.

Hruska-Hageman AM, Wemmie JA, Price MP, Welsh MJ. Interaction of the synaptic protein PICK1 (protein interacting with C kinase 1) with the non-voltage gated sodium channels BNC1 (brain Na^+ channel 1) and ASIC (acid-sensing ion channel). *Biochem J* 361: 443–450, 2002.

Kellenberger S, Schild L. Epithelial sodium channel/degenerin family of ion channels: a variety of functions for a shared structure. *Physiol Rev* 82: 735–767, 2002.

Krishtal O. The ASICs: signaling molecules? Modulators? *Trends Neurosci* 26: 477–483, 2003.

Krishtal OA, Osipchuk YV, Shelest TN, Smirnoff SV. Rapid extracellular pH transients related to synaptic transmission in rat hippocampal slices. *Brain Res* 436: 352–356, 1987.

Lalo U, Pankratov Y, North RA, Verkhratsky A. Spontaneous autocrine release of protons activates ASIC-mediated currents in HEK293 cells. *J Cell Physiol* 212: 473–480, 2007.

Lingueglia E, de Weille JR, Bassilana F, Heurteaux C, Sakai H, Waldmann R, Lazdunski M. A modulatory subunit of acid sensing ion channels in brain and dorsal root ganglion cells. *J Biol Chem* 272: 29778–29783, 1997.

Lisman J, Schulman H, Cline H. The molecular basis of CaMKII function in synaptic and behavioural memory. *Nat Rev Neurosci* 3: 175–190, 2002.

Llinás R, Gruner JA, Sugimori M, McGuinness TL, Greengard P. Regulation by synapsin I and Ca(2+)-calmodulin-dependent protein kinase II of the transmitter release in squid giant synapse. *J Physiol* 436: 257–282, 1991.

MacDermott AB, Role LW, Siegelbaum SA. Presynaptic ionotropic receptors and the control of transmitter release. *Annu Rev Neurosci* 22: 443–485, 1999.

Mennerick S, Que J, Benz A, Zorumski CF. Passive and synaptic properties of hippocampal neurons grown in microcultures and in mass cultures. *J Neurophysiol* 73: 320–332, 1995.

Mennerick S, Zorumski CF. Paired-pulse modulation of fast excitatory synaptic currents in microcultures of rat hippocampal neurons. *J Physiol* 488: 85–101, 1995.

Miesenbock G, De Angelis DA, Rothman JE. Visualizing secretion and synaptic transmission with pH-sensitive green fluorescent proteins. *Nature* 394: 192–195, 1998.

Monyer H, Sprengel R, Schoepfer R, Herb A, Higuchi M, Lomeli H, Burnashev N, Sakmann B, Seeburg PH. Heteromeric NMDA receptors: molecular and functional distinction of subtypes. *Science* 256: 1217–1221, 1992.

Moulder KL, Meeks JP, Shute AA, Hamilton CK, de Erausquin G, Mennerick S. Plastic elimination of functional glutamate release sites by depolarization. *Neuron* 42: 423–435, 2004.

Palmer MJ, Hull C, Vigh J, von Gersdorff H. Synaptic cleft acidification and modulation of short-term depression by exocytosed protons in retinal bipolar cells. *J Neurosci* 23: 11332–11341, 2003.

Price MP, Lewin GR, McIlwrath SL, Cheng C, Xie J, Heppenstall PA, Stucky CL, Mannsfeldt AG, Brennan TJ, Drummond HA, Qiao J, Benson CJ, Tarr DE, Hrstka RF, Yang B, Williamson RA, Welsh MJ. The mammalian sodium channel BNC1 is required for normal touch sensation. *Nature* 407: 1007–1011, 2000.

Price MP, McIlwrath SL, Xie J, Cheng C, Qiao J, Tarr DE, Sluka KA, Brennan TJ, Lewin GR, Welsh MJ. The DRASIC cation channel contributes to the detection of cutaneous touch and acid stimuli in mice. *Neuron* 32: 1071–1083, 2001.

Price MP, Snyder PM, Welsh MJ. Cloning and expression of a novel human brain Na^+ channel. *J Biol Chem* 271: 7879–7882, 1996.

Priller C, Bauer T, Mitteregger G, Krebs B, Kretzschmar HA, Herms J. Synapse formation and function is modulated by the amyloid precursor protein. *J Neurosci* 26: 7212–7221, 2006.

Rhee JS, Betz A, Pyott S, Reim K, Varoqueaux F, Augustin I, Hesse D, Sudhof TC, Takahashi M, Rosenmund C, Brose N. Beta phorbol ester- and diacylglycerol-induced augmentation of transmitter release is mediated by Munc13s and not by PKCs. *Cell* 108: 121–133, 2002.

Rosenmund C, Clements JD, Westbrook GL. Nonuniform probability of glutamate release at a hippocampal synapse. *Science* 262: 754–757, 1993.

Rosenmund C, Stevens CF. Definition of the readily releasable pool of vesicles at hippocampal synapses. *Neuron* 16: 1197–1207, 1996.

Sanhueza M, McIntyre CC, Lisman JE. Reversal of synaptic memory by Ca^{2+}/calmodulin-dependent protein kinase II inhibitor. *J Neurosci* 27: 5190–5199, 2007.

Sutherland SP, Benson CJ, Adelman JP, McCleskey EW. Acid-sensing ion channel 3 matches the acid-gated current in cardiac ischemia-sensing neurons. *Proc Natl Acad Sci USA* 98: 711–716, 2001.

Vessey JP, Stratis AK, Daniels BA, Da Silva N, Jonz MG, Lalonde MR, Baldridge WH, Barnes S. Proton-mediated feedback inhibition of presynaptic calcium channels at the cone photoreceptor synapse. *J Neurosci* 25: 4108–4117, 2005.

Waldmann R. Proton-gated cation channels-neuronal acid sensors in the central and peripheral nervous system. *Adv Exp Med Biol* 502: 293–304, 2001.

Waldmann R, Champigny G, Bassilana F, Heurteaux C, Lazdunski M. A proton-gated cation channel involved in acid-sensing. *Nature* 386: 173–177, 1997.

Waldmann R, Champigny G, Voilley N, Lauritzen I, Lazdunski M. The mammalian degenerin MDEG, an amiloride-sensitive cation channel activated by mutations causing neurodegeneration in *Caenorhabditis elegans*. *J Biol Chem* 271: 10433–10436, 1996.

Waxham MN, Malenka RC, Kelly PT, Mauk MD. Calcium/calmodulin-dependent protein kinase II regulates hippocampal synaptic transmission. *Brain Res* 609: 1–8, 1993.

Wemmie JA, Askwith CC, Lamani E, Cassell MD, Freeman JH Jr, Welsh MJ. Acid-sensing ion channel 1 is localized in brain regions with high synaptic density and contributes to fear conditioning. *J Neurosci* 23: 5496–5502, 2003.

Wemmie JA, Chen J, Askwith CC, Hruska-Hageman AM, Price MP, Nolan BC, Yoder PG, Lamani E, Hoshi T, Freeman JH Jr, Welsh MJ. The acid-activated ion channel ASIC contributes to synaptic plasticity, learning, and memory. *Neuron* 34: 463–477, 2002.

Wemmie JA, Coryell MW, Askwith CC, Lamani E, Leonard AS, Sigmund CD, Welsh MJ. Overexpression of acid-sensing ion channel 1a in transgenic mice increases acquired fear-related behavior. *Proc Natl Acad Sci USA* 101: 3621–3626, 2004.

Wemmie JA, Price MP, Welsh MJ. Acid-sensing ion channels: advances, questions and therapeutic opportunities. *Trends Neurosci* 29: 578–586, 2006.

Wierda KD, Toonen RF, de Wit H, Brussaard AB, Verhage M. Interdependence of PKC-dependent and PKC-independent pathways for presynaptic plasticity. *Neuron* 54: 275–290, 2007.

Xiong ZG, Chu XP, Simon RP. Ca^{2+}-permeable acid-sensing ion channels and ischemic brain injury. *J Membr Biol* 209: 59–68, 2006.

Xiong ZG, Zhu XM, Chu XP, Minami M, Hey J, Wei WL, MacDonald JF, Wemmie JA, Price MP, Welsh MJ, Simon RP. Neuroprotection in ischemia: blocking calcium-permeable acid-sensing ion channels. *Cell* 118: 687–698, 2004.

Yermolaieva O, Leonard AS, Schnizler MK, Abboud FM, Welsh MJ. Extracellular acidosis increases neuronal cell calcium by activating acid-sensing ion channel 1a. *Proc Natl Acad Sci USA* 101: 6752–6757, 2004.

Zha XM, Wemmie JA, Green SH, Welsh MJ. Acid-sensing ion channel 1a is a postsynaptic proton receptor that affects the density of dendritic spines. *Proc Natl Acad Sci USA* 103: 16556–16561, 2006.

Zhong N, Beaumont V, Zucker RS. Calcium influx through HCN channels does not contribute to cAMP-enhanced transmission. *J Neurophysiol* 92: 644–647, 2004.

Zucker RS, Regehr WG. Short-term synaptic plasticity. *Annu Rev Physiol* 64: 355–405, 2002.